PREPARATION AND MECHANICAL BEHAVIOUR OF POWDER METALLURGICAL LEAD-BASE PARTICULATE COMPOSITES

By

PRALHADRAO BHAUSAHEB KADAM

To

My Wife Vijaya
and
daughter Priyadarshani

ME=1979—D-KAD-PRE

I.I.T Kanpur.
Submitted on 6.12.22
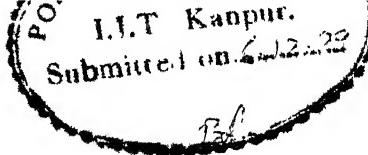
CERTIFICATE

This is to certify that this work "Preparation
and Mechanical Behaviour of Powder Metallurgical Lead-
base Particulate Composites", has been carried out by
Mr. Pralhadrao Bhausaheb Kadam under our supervision,
and it has not been submitted elsewhere for a degree.

G.S. MURTY
Professor

G.S. UPADHYAYA
Professor

M.L. VAIDYA
Asstt. Professor

Department of Metallurgical Engineering
Indian Institute of Technology
Kanpur, India

ACKNOWLEDGEMENTS

I take this opportunity to thank sincerely Dr. G.S. Murty, Dr. G.S. Upadhyaya and Dr. M.L. Vaidya for their able guidance, lively discussions and suggestions throughout the work.

Special thanks are due to Dr. Satyanarayan and Dr. Chaudhari of Metallurgy Department, College of Engineering, Poona for their encouragement to take up post-graduate studies leading to doctoral degree.

Grateful acknowledgements are due to Quality Improvement Programme, Government of India, and Department of Technical Education, Government of Maharashtra for providing me necessary funds and facilities respectively.

I would like to thank all my friends, Sarvashri Sodhi, Ramamurty, Adgaonkar, Kashyap, N. Singh and Kale who helped me in my work.

Mr. R.N. Srivastava is to be congradulated and thanked for excellent typing. Mr. Panesar is thanked for his help in preparing the drawings.

Last but not least, my soulful thanks are due to my wife, Sou Vijaya and my daughter, Priyadarshni who have encouraged me and sustained with patience my absence from home all through the programme.

<div style="text-align: right">Pralhadrao Bhausaheb Kadam</div>

TABLE OF CONTENTS

LIST OF TABLES

LIST OF FIGURES

LIST OF SYMBOLS

T_p — Temperature of processing (°K)

T_R — Recrystallisation temperature (°K)

μm — Micron (10^{-4} cm)

λ — Mean free path

A — Constant

B — Constant

σ_y — Tensile yield stress

D — Interparticle distance/grain size

σ_c — Compressive yield stress

σ_t — Tensile yield stress

σ_i — Internal stress

τ_a — Applied shear stress

τ_e — Effective shear stress

τ_i — Internal shear stress

τ_m — Matrix shear stress

τ_p — Orowan stress (particle strengthening contribution)

τ_s — Substructural strengthening contribution

τ_t — Textural strengthening stress contribution

$\overset{\circ}{A}$ — Angstron (10^{-8} cm)

ε — Strain

$\dot{\varepsilon}_s$ — Steady state creep rate

γ — Shear strain

$\dot{\gamma}_s$ — Steady state shear strain rate

R	—	Gas constant
T	—	Absolute temperature in ($^\circ$K)
T_m	—	Absolute temperature of melting ($^\circ$K)
K	—	Material constant
d	—	Average particle diameter/grain diameter
b	—	Burger's vector
G_m	—	Shear modulus of material
G_p	—	Shear modulus of particle (dispersoid)
D_o	—	Diffusion coefficient
Ω	—	Atomic volume
n_a	—	Apparent stress exponent (a constant)
n_e	—	Effective stress exponent
Q_a	—	Apparent activation energy
Q_{SD}	—	Activation energy for self diffusion
τ_T	—	Total shear strength
$\sigma^C_{0.2\%}$	—	Offset yield strength in compression
$\sigma^T_{0.2\%}$	—	Offset yield strength in tension

ABSTRACT

Three types of Lead base particulate composites,
namely, P/M Lead (containing PbO particles), Pb-Zn and
Pb-Al$_2$O$_3$ with dispersoid size - ranging between 0.1 to
2 μm, were prepared using powders of Lead (atomised), Zinc
(atomised) and Alumina. In the case of Pb-Zn and Pb-Al$_2$O$_3$
composites, the dispersoid content was varied in the range
of 2.5 to 7.5 V/O and these were prepared by mixing of
powders followed by consolidation using one or more of
techniques such as compaction, sintering, extrusion and
swaging.

It was observed that the Lead-base composites can
be compacted to a density level of 98 % . (of the theore-
tical density-TD) by room temperature compaction using
a pressure of 384 MPa (high pressure). When the compaction
pressure was 128 MPa (comparatively low pressure), the
green density achieved was about 74 % . (TD). It can be
further improved by sintering at 280°C (≈ 0.92 Tm) to a
level of 89.5 % . (TD) or by extrusion to a level of
87 %' of TD.

A combination of low compaction pressure, extrusion
and swaging resulted in a product of density more than

• Tm — Absolute temperature of melting (°K).

97. (TD) but the product exhibited non-uniform porosity.
Further, a combination of low pressure compaction, sintering
and extrusion resulted in a product of higher density
($>$ 98 pct. TD) and more uniform porosity distribution.
However, the products of the latter combination of
consolidation techniques had exhibited significantly
different yield strength values (SD effect) in compression
and tension. The extent of the SD effect was influenced
by the nature of dispersoid, such that Zn containing
composites have shown maximum SD effect amongst all the
products. The SD effect can be reduced by increasing the
compaction pressure during the consolidation stage. The
observed SD effect in these composites is the manifestation
of the combined effect of the matrix-particle interface
bond strength and residual stresses of thermal and mechanical
origin.

In the dispersoid size range studied all
the Lead-base composites showed strengthening over Lead
(prepared via conventional route) and the extent of strengthening was observed to depend on the nature of dispersoid.
Pb-Zn, Pb-PbO and Pb-Al$_2$O$_3$ composites exhibited strengthening

in the increasing order. Further, the strengthening increased with the volume fraction of the dispersoid in the case of $Pb-Al_2O_3$, whereas opposite effect was observed in Pb-Zn composites. The strengthening or weakening observed in these composites is explained in terms of indirect particle effect on parameters, such as σ_i and K_y in the Hall-Petch type relation, the nature of the dispersoid alongwith its distribution and the temperature of testing.

The threshold stress for steady-state creep was observed in Pb - 2.5 V/O PbO and $Pb-5V/O\ Al_2O_3$ composites below $150^\circ C$, whereas it was absent in Pb-5 V/O Zn composites. Two distinct stress exponent regions with different activation energies were observed over a shear strain rate range of 10^{-7} to 10^{-4} sec^{-1}. In the low stress exponent region, grain boundary sliding appears to be the rate controlling mechanism, whereas climb controlled dislocation creep is the operative mechanism in the other region.

CHAPTER I

INTRODUCTION

The world of materials has expanded considerably by recognizing the fact that it is possible to produce solids of desirable overall properties by mixing intimately solids of dissimilar nature. Such intimate mixtures are called "composites". The well known examples are fibre glass reinforced plastics, concrete and thoria dispersed nickel. The advantages of such materials are several, e.g., improved mechanical strength, high strength to weight ratio, enhanced creep resistance, better physical properties etc. Of course, all these improvements in properties need not necessarily be obtained in a single composite.

For composite preparation generally, a base (matrix) material, which may be a metal or nonmetal is chosen to which other solids of various shape and size are added. Depending upon the shape of the added solids, these composites are grouped into, (i) particulate or (ii) fibre types. The particulate composites contain near rounded particles (called dispersoids) whereas the fibre types contain long thin fibres. The fibres may be continuous or discontinuous in nature.

A considerable amount of work is going on in the field of composites using metals as matrix materials. It

has a dual aim of improving our understanding regarding their behaviour and developing new materials. The work reported in this thesis is on Lead base particulate composites. In this introductory chapter, the scope of the work is presented after reviewing relevant literature on metal-matrix particulate composites. The arrangement of the chapter is as follows: Section 1.1 presents a brief description of powder metallurgy (P/M) route of processing particulate composites, since it is the route adopted for making composites used in the present investigation. Section 1.2 describes mechanical behaviour of various classes of metal-matrix particulate composites. In Section 1.3, a brief review of literature on Lead base composites is presented. Finally, Section 1.4 outlines the objectives and scope of the present study.

1.1 P/M Route of Processing Metal-Matrix Particulate Composites

Particulate composites can be prepared in several ways. (i) They may be prepared by casting followed by mechanical working and suitable heat-treatment, such as precipitation hardening, internal oxidation or internal nitridation. (ii) They may be obtained by mixing solid insoluble dispersoids during molten stage of matrix metal and subsequently casting followed by mechanical working. (iii) They may be developed through P/M route involving

mixing of matrix metal and dispersoid powders followed by consolidation through compaction, extrusion, rolling, swaging etc.

P/M route is the most versatile of all the processes in the sense that one can obtain composites of any matrix metal with any type of dispersoid. The problem of uniform dispersion of the dispersoid, though exist in P/M composites also, it is less difficult to surmount. General details of P/M route are reviewed in the following sections.

1.1.1 Mixing

Mixing of matrix metal powder with that of dispersoid material is the first step in the P/M route. In order to bring out effectiveness of dispersoids, it is necessary to produce very intimate mixture of matrix metal and dispersoid particles. Several techniques have been adopted to achieve intimate mixing.

Surface oxidation[1] involves obtaining metal powders with an adherent self oxide layer on individual particles. Such powders are produced by air atomisation of liquid metals or mechanical milling of solid metal. The thickness of the oxide layer on atomised or milled powders is approximately 100 $\overset{o}{A}$. This thickness can be further increased by controlled oxidation in an oxygenated atmosphere at an elevated temperature. This technique was first used[2] in processing Aluminium-Alumina oxide composites, commonly,

called SAP. The total oxide contents of the composite made out of such powders depends upon the particle size of the powder and subsequent oxidation treatment, if any.

Internal oxidation[3] involves preferential oxidation of solute element in a dilute solid solution alloy powder particles. For preferential oxidation of the solute elements, it is necessary that solute metal oxide has a higher negative heat of formation than that of the matrix metal oxide. The composite produced by using internally oxidised powders is essentially an oxide dispersed composite. The process has been commercially adopted both for refractory[4] and metal base composites[5].

Reduction technique[6] involves first step of preparing an intimate mixture of the matrix and dispersed oxides and then selectively reducing the matrix oxides prior to conventional powder consolidation. The preferential reduction of matrix metal oxide needs lower stability than that of the dispersed oxide. The reduction is carried out in hydrogen atmosphere. The process has been commercialised for Nickel-Thoria composites[7].

Mechanical mixing[8] technique is self explanatory in its terminology. The mixing of matrix and dispersoid powders is achieved through such automatic equipments as ball milling, high speed blending machine etc. The technique is versatile in the sense that dispersoids of different nature

can be mixed with the matrix metal powder. For proper mixing, it is generally necessary to maintain a minimum particle size ratio of 20:1 for matrix metal as to dispersoid powders.

Mechanical alloying[9] is the latest modification of mechanical mixing technique. The composite powders are processed in attritor grinding mills. These are high energy driven ball mills in which the charge of ball and powder is held in a satisfactory, vertical, water cooled tank and agitated by impellers radiating from a rotating central shaft. This technique produces homogeneous intimately dispersed powder mixtures.

Shotting technique[10] utilises insolubility of a dispersoid material in the solid state and a partial solubility of the solute in the liquid state of the matrix metal. A dilute liquid solution of the matrix metal and the dispersoid is atomised. The rapid chilling of the small liquid droplets (shotting) results in a fine dispersion of insoluble dispersoid phase. This process is restricted to metal-metal and metal-intermetallic compounds only[11].

Salt decomposition[12] technique utilises the decomposition of salts which are capable of forming a refractory oxide on fine metal powder. Salts commonly utilised in this process are nitrates, oxalates and sulphates. The technique has been used for Nickel-Thorium oxide (TD-Nickel) composite powders.

1.1.2 Consolidation of pre-mixed powders

Consolidation of the pre-mixed powders is the next step in the production of particulate composites. The aim of consolidation is to achieve a good binding between individual particles of the pre-mixed powder and produce a dense product. Other considerations are shaping up the product, improvement of the matrix grain size, uniform distribution of dispersoid particles. Variety of techniques are used for the purpose e.g., compaction (pressing), extrusion, rolling or swaging. These may be carried out in cold (temperature of processing, T.P < T.R, where TR is recrystallization temperature) or hot (TP > TR) state. When processing is done in cold state, it is invariably followed by sintering. Hot processing does not require further sintering, since the sintering effects will be concurrent with the deformation.

The success of any consolidation technique lies in controlling process variables. For example, in compaction these variables are pressure of compaction, nature of compaction (whether unidirectional or iso-static), die wall friction etc. In case of extrusion, extrusion ratio, extrusion speed, die angle and wall friction are the process variables. Similarly, there are other process variables in rolling or swaging. If the processing is done in hot state, temperature of processing becomes an important variable. In case the products are sintered, sintering temperature and time become important variables.

Consolidated composites may be re-processed using such techniques as extrusion, rolling, swaging etc. This is done to improve dispersoid dispersion, refine matrix grain size or strain harden the matrix phase and reduce the porosity content of the material further.

1.2 Mechanical Behaviour of Metal-Matrix P/M Particulate Composites

The principal aim of developing metal-matrix particulate composites is to obtain materials with better mechanical properties. Mechanical behaviour of metals is profoundly affected by dispersing particles of other materials into them. In this section, important changes in their mechanical behaviour due to dispersoid additions that have been reported are reviewed.

Before reviewing, it is convenient to classify the various metal-matrix particulate composites into two broad groups. The grouping has been done on the basis of dispersoid particle size and volume fraction ranges (Table 1.1). These are two parameters which affect the mechanical behaviour of these composites to a large extent.

1.2.1 Aggregate type (Particle size greater than 2 μm)

These are high volume fraction composites containing large sized dispersoids. In these composites, it has been possible to achieve strength levels 15 to 17 times over

that of matrix metal. There are several examples of this
kind[13,14]. Cobalt-base composites[13] with WC (tungsten
carbide) as the dispersoid phase is the principal example of
this type. The strengthening has been attributed to two
factors, viz. (i) plastic constraint exerted by hard
dispersoid particles on the matrix phase and (ii) load sharing
by the dispersoid phases. In addition to these factors,
thermal residual stresses, arising out of differences in
thermal expansion coefficients of matrix and dispersoid phases,
have also been invoked to explain the strengthening[15].
Thermal residual stresses would be large, provided (i) thermal
coefficient differences between matrix and dispersoid and
(ii) the dispersoid particle size are large.

Besides Co-WC system, the other composites that
have been extensively studied are Cu-base[16] where particles
of Cr, Fe, Mo, graphite, and Al_2O_3 have been added. The
strengthening achieved in these composites is expressed as
follows:

$$\sigma_y = - A \log \lambda + B . \qquad (1.1)$$

where σ_y is tensile yield strength, λ is mean free path
between the particles and A and B are material constants.

Though considerable strengthening can be achieved
in these types of composites, ductility values are extremely
poor. These are even less than 1%[13]. Low ductility
precludes the use of these composites as structural materials.

Such materials are mostly used in cutting and wear resistance applications. The hardness values are retained upto a fairly high temperature.

1.2.2 Dispersion type (particle size less than 0.1 μm)

These are low volume fraction particulate composites with very fine particles (< 0.1 μm) dispersed in metal-matrix. By uniform dispersion of fine particles, it has been possible to improve yield strength of matrix metals by a factor of 5 to 8. Such strengthening effects have been reported in SAP[2,17], TD-Nickel[18], $Cu-Al_2O_3$[5, 19], $Cu-SiO_2$[5, 19] and $Fe-Al_2O_3$[20] particulate composites. Strengthening is retained at elevated temperatures too.

Several mechanisms have been proposed to explain the dispersion strengthening effects in these composites[21,22,23]. Basically, the strengthening is due to direct particle-dislocation interactions. According to Orowan mechanism[21], the stress (τ_p) necessary for a dislocation to by pass the dispersoid particles is given by

$$\tau_p = \frac{G_m b}{\lambda} \qquad (1.2)$$

where G_m is the shear modulus of the matrix, b is Burgers vector of the dislocation and λ is the inter-particle distance. A more rigorous expression for the Orowan stress has been suggested by Ashby[22]. Another mechanism based on stress-induced particle shear or fracture has been

proposed by Ansell[23] to account for the dispersion streng-thening of such fine particulate composites.

On the basis of any of these mechanisms, the inter-particle distance plays an important role in the strengthening of the composites. It follows that for a given volume fraction of the dispersoids, smaller the particle size, smaller would be interparticle distance values and hence greater would be strengthening effect. For larger particles, one has to increase the volume fraction to achieve same value of λ and achieve similar level of strength. It is preferable to disperse smaller volume fractions of smaller particles. But there are practical problems in achieving fine dispersions with smaller particles. Further, there is a greater tendency for finer particles to agglomerate and thus affect their uniform distribution in matrix material. That brings in the role of preparation of these composites. The uniformity of distribution is better if the composites are obtained through internal oxidation (or nitridation) technique.[24] Mechanical mixing is better suited for larger sized particles.

Strengthening in some of these composites has been improved[25-27] by suitable thermo-mechanical treatments (TMT). The source of additional strengthening in these cases is attributed to indirect effects of TMT on matrix structure. TMT gives rise to fine grains and dislocation substructure. The total strengthening is then expressed as:

$$\tau_T = \tau_m + \tau_p + \tau_s \qquad (1.3)$$

where τ_m is matrix shear strength, τ_p is Orowan type contribution to strength by the particles and τ_s is the substructural strengthening. The strength achieved through TMT may be as high as 10 times or more than that of the matrix metal.

As far as strength values are concerned, there is a significant difference in yield values in tension and compression (asymmetric behaviour) reported in case of an important composite of this group, viz. TD-Nickel[28]. Compressive yield strength of this composite differs from tensile one by an amount as much as 50%. Such strength differential is known as SD effect. The extent of this effect is reduced or eliminated[29] through suitable solid solution alloying of the matrix phase. The explanation of such an effect is given in terms of particle-matrix interface bond strength[28]. Such a behaviour is notably absent in SAP material[28].

As far as the ductility values are concerned, these composites are more ductile than the aggregate type but the values are still low. They range between 5 to 10%. TMT improves the ductility somewhat. Mechanically mixed composites are more ductile than those obtained through internal oxidation technique[24].

In some of these composites, so called "ductilization" effect is reported, e.g., in Cr-base[30] composites containing tantalum and titanium as the dispersoid materials. The ductility of Cr is reported to have improved from 0 to 20%. The ductilization has been attributed in one model[31] to scavenging effect of the dispersoids on dissolved nitrogen and oxygen in the base material, while in other model[32] the same effect has been explained on the basis of generation of dislocations at dispersoid-matrix interface to accommodate stress inhomogeneity around the particle during deformation or relaxation of triaxiality around tips of cracks near particle-matrix interfaces.

One of the significant effects obtained in these composites is the retention of strength at elevated temperatures. As a consequence of it, creep properties are considerably improved. There is a significant drop in creep rates (3-5 orders of magnitudes). However, the stress sensitivity of steady state creep rates is increased i.e. to say in the general expression for steady state creep rate, $\dot{\varepsilon}_s = A \sigma^{n_a} \exp(- Q_a/RT)$ where, $\dot{\varepsilon}_s$, is the steady state creep rate, A is a constant, σ is the applied stress, n_a is the stress sensitivity factor, Q_a is apparent activation energy, values are significantly higher[33-35]. Also, the apparent activation energy values are higher. Table 1.2 gives some of the observed values of Q_a and n_a. In certain composites of this group, a threshold stress below which

creep rates become negligibly small has been observed[36].
The creep resistance of these composites is reported[37] to
be sensitive to grain morphology also.

A number of possible dislocation creep mechanisms
have been proposed to account for the creep behaviour of
dispersion strengthened composites of this group. The basis
of most of these models is the original proposal by Ansell
and Weertman[38]. In this proposal, the stress exponent 'n'
for the steady state creep rate is given as 4.5 which
obviously does not explain the higher values obtained in
several cases. Also, the activation energy values proposed
for the process are close to self diffusion activation
energy values. The model by Ansell and Weertman has been
modified[39-41] by others by invoking the concept of
effective stress. The effective stress operating during
creep deformation has been visualized as equal to $(\tau_a - \tau_i)$
where τ_a is the applied shear stress and τ_i is the long
range internal stress in the material through different
sources. τ_i in dispersion strengthened composites is
generally observed to be large and therefore the creep
rate is drastically reduced and in certain cases brought
to zero below a certain stress level. Both high stress
exponent and high activation energies observed have been
accounted[39-41] in terms of high τ_i values.

1.2.3 Dispersion type (Particle size between 0.1 to 2 μm)

Generally, dispersion strengthened composites have been confined to dispersoid size range below 0.1 μm. There are a few composites reported in the literature[42,43,44] in the particle size range of 0.1 to 2 μm grouped under dispersion type. These are mostly CPH metal-matrix composites. The systems that have been extensively studied are Zn-based[42,43] composites containing Al_2O_3, W, C and ZnO as dispersoids and Cd-base[44] composites containing B and W as the dispersoids. In this section the mechanical behaviour of these composites are reviewed.

In case of Zn-composites[43] containing W and Al_2O_3, strengthening has been reported below 0.3 T_m and above 0.7 T_m with respect to Zinc prepared from powder metallurgy. Strengthening is not compared explicitly with respect to that of Zinc obtained through the conventional route of casting and mechanical working. It has been proposed[43] that the strengthening below 0.3 T_m is due to particles acting as dislocation sources and grain boundaries acting as effective barriers to dislocation motion thereby leading to rapid work-hardening. Above 0.3 T_m recovery processes are dominant, which causes weakening of the composites with respect to pure Zinc. The weakening observed in Zn-base composites is explained on the basis of the particles acting as dislocation sources[43].

Cd-base[44] composites containing B and W have shown strengthening with respect to that of cast cadmium. The strength improvement is about 3.5 times, at room temperature[44]. The strengthening has been explained on the basis of combined effect of grain size and particle strengthening. Grain size strengthening is given by a Hall-Petch[45,46] type relationship and particle strengthening (τ_p) by an empirical expression, $\tau_p = kd^{-0.1}$, where k is a material constant and d is average particle diameter of the dispersoids. It has been shown that P/M cadmium also possesses strength greater than the cast Cd. In that case the strengthening is attributed to grain size and crystallographic texture developed due to mechanical working. Yield strength is given by $\tau_T = \tau_m + \tau_{Te}$ where τ_m is grain size strengthening through Hall-Petch type relationship and τ_{Te} is texture strengthening contribution. Cd-W composites containing 30 V/O W exhibit weakening above $0.5\ T_m$ with respect to P/M cadmium. The explanation for such a weakening is again based on dispersoid particles acting as dislocation sources[43] and recovery being dominant above $0.5\ T_m$.

As far as ductility values are concerned, all the Zinc composites, except those of carbon, have shown[42] : . in ductility over that of P/M Zinc. This has been attributed to two factors namely, (i) preexisting

internal stress through thermal sources[15] and (ii) initiation of multiple slip due to stress concentration developed at the particle matrix interface[47]. In case of Cd-base composites such ductilization is not reported. As a matter of fact, ductilities are poor in these cases. However, here strain softening is observed. The phenomenon of strain softening is attributed to strong preferred orientation[44,48] obtained in Cd-base composites whereas in Zn-composites, it is again based on internal stresses[15,42] and duplex slip mechanisms[47].

No creep studies are reported in this type of composites. Only in case of Zn-composites[43] some data are reported as regards strain-rate vs. stress based on compression testing. An important feature of these data is the indication of threshold stress below which strain rates are negligibly small. This observation is somewhat similar to that of fine dispersion type composites. There is a lack of data at low strain rate levels for such composites.

1.3 Mechanical Behaviour of Lead Base P/M Particulate Composites

The results on Lead-base particulate composites are presented separately in this section, partly because of the direct relevance of these results to the present work

on Lead-base composites and partly due to lack of proper information regarding the dispersoid particle sizes in most of the reported studies.

Several types of dispersoids have been added[49-58] to improve the strength of Lead. Strength improvement by a factor approximately 3.6 has been reported at room temperature ($\simeq$ 0.5 T_m for Lead) by 15 v/o PbO.[49] In case of composites containing Al_2O_3 (0.005 to 0.03 µm) upto 5 volume percent, the strength was improved by 5 times over that of Lead in extruded state[50]. However, in the latter case, the processing was very difficult and rather uneconomical vis-a-vis the degree of strengthening achieved. In case of a composite containing metallic dispersoids, viz., Sb[51], strength is shown to be superior to that in Pb-PbO composites upto 150°C ($\simeq$ 0.7 T_m). However, above 0.7 T_m, Pb-PbO composites were found to be superior. In certain composites[52,53,54] strength has been shown to be sensitive to strain rate of testing, which has been attributed to dynamic recovery process.

Strengthening in Lead-base composites is explained[45,46] on the basis of a Hall-Petch type relationship proposed as follows:

$$\sigma_y = \sigma_o + kD^{-1/2} \qquad (1.4)$$

where σ_o and k are material constants and D is either mean free path (MFP), grain size or dislocation particle network

size[55,56]. MFP is affected by the original Lead-powder
size used for preparing the composites. For a given oxide
content, finer the particle size of the original Lead powder,
smaller is the MFP in the product. Further, MFP is aniso-
tropic in character in the sense that it is different in
the transverse direction than in the longitudinal. This
anisotropy in MFP is due to processing.

Ductility in these composites has been shown to
decrease with increasing volume fractions of dispersoids.
It also depends upon the nature of the dispersoids. For
Pb-PbO composites, the values range from 7 to 23%[49]. For
other composites, it is reported to be less than 7%. As
far as creep behaviour is concerned, the only reported study
(in recrystallised state) is on Pb-PbO (2.5 V/O). This
study has revealed that the creep rates could be decreased
by 3 orders of magnitude[57] by dispersing oxide dispersoids.
It is observed that the creep resistance is favoured by a
large volume fraction of oxide concentrated at the boundaries
which pin down their movement. The stress dependence of
steady state creep rate has been shown[58] to vary from 6
to 27 as against that of pure Lead between 1 to 5[58].
However, the high value of exponent appears to be a
function of processing. In recrystallized state of the
composites the value of the exponent is 5[57]. The creep
behaviour is explained on the basis of a modified Ansell-
Weertman[38] model.

1.4   Scope of the Present Study

It is fairly well established that the mechanical behaviour of metal-matrix particulate composites is profoundly affected by size and volume fraction of the dispersoid particles. Most of the particulate composites that have been investigated and developed commercially lie either in the particle size range below 0.1 μm or above 2 μm. In the entire spectrum of particle sizes, there appears to be a lack of studies in range of 0.1 to 2 μm. The reported cases are a few in number and the mechanical behaviour of such composites is not well understood. There are conflicting observations of both strengthening and weakening. The systems that have been studied in this range mostly belong to CPH metal base. The CPH metals have their own pecularities in terms of available slip systems whereas the FCC metals have no such limitation.

The present study has therefore, been undertaken on composites containing particles in the size range of 0.1 to 2 μm. FCC metal, namely, Lead has been chosen as the matrix-metal. Keeping in view two essential requirements for the choice of dispersoid particles, namely, (i) their inertness and (ii) higher strength with respect to matrix-metal Lead, two types of dispersoids have been added. These are Zinc and Alumina. These two dispersoids differ in their basic nature i.e.. the former is metallic,

and the latter nonmetallic in nature. They also differ in their relative hardness values. Zn is softer than Al_2O_3. The differences in dispersoid nature are further expected to affect microstructure of these composites and consequently their mechanical behaviour.

P/M route has been chosen for the preparation of composites in the present study, since it is considered to be a convenient and more effective route of making such composites. When the powder parameters such as particle size and nature of dispersoid chosen are different, the composite characteristics such as porosity, microstructure and compressive yield strength would be different. Similarly, processing parameters such as thermal and mechanical working inclusive of powder compaction and deformation processing would alter these characteristics and thereby the mechanical behaviour of composites.

In view of the above broad objectives, an exploratory study involving preparation and mechanical behaviour of Lead-base particulate composites prepared through P/M has been made in the present investigation. It has been tried to evolve a suitable processing method varying various processing parameters and to establish room and high temperature mechanical behaviour including creep of these Lead-base composites.

Table 1.1

Classification of particulate composites

Type	Particle size range (µm)	Particle volume fraction (f)
Aggregate	above 2.0	0.2 to 0.9
Dispersion		
(a)	less than .100 (fine particle)	0.01 to 0.1
(b)	0.1 to 2.0 (coarse particle)	upto 0.3.

Table 1.2

Activation energies (Q_a) and stress exponent (n_a) values for dispersion type particulate composites (< 0.1 µm)

Composite	Apparent activation energy (Q_a) kcal/mol	Apparent stress exponent (n_a)
SAP	150-180	10
TD-Nickel	190	40
Ni-Cr-ThO$_2$	92	24

CHAPTER II

EXPERIMENTAL PROCEDURES

The various procedures with their relevant experimental details regarding the (i) preparation of composites (ii) porosity measurement (iii) microstructural observations and (iv) mechanical testing consisting of compression, tension and creep are presented in above order in this chapter.

2.1 Materials

Three kinds of powders were used in the present investigation, viz., Lead, Zinc and Alumina. The atomized Lead and Zinc powders were supplied by M/s Khosla Metal Powders Ltd. and Alumina powder, designated Linde A, was obtained from Union Carbide Corporation of U.S.A.

In the as received condition, Lead powder contained its self oxide or pre-existing oxide (PbO) 1% by weight. Average particle sizes of supplied Lead, Zinc and Alumina powders were 38, 30 and 1 μm respectively. In order to have achieved the size upto 1 μm, Zinc powder was reduced in a fluid mill which works on a cyclone system where the pressures at powder and air inlet ends were maintained at 8 kg/cm^2 and 6 kg/cm^2 respectively. The air compressor was regulated at 100 kg/cm^2. Fine particle sizes attained in zinc were in the range of 1.2 to 2 μm. Most of the Zinc powder size was in the lower range. Zinc and Alumina were used separately as the dispersoids in this investigation. Particle sizes were initially determined on Fisher-Sub-sieve Analyser and finally through optical measurements.

2.2 Preparation of Lead-base P/M Particular Composites

Processing of composites consisted of the following stages: (i) Mixing of powders, (ii) Compaction, (iii) Vacuum sintering, (iv) Extrusion, (v) Swaging and (vi) Annealing.

2.2.1 Mixing of powders

The Lead powder was screened through 200 mesh sieve before filling in die for compaction. The required volume percentages of dispersoids (Zinc or Alumina) and matrix powder (Lead) were weighed in appropriate proportion on a single pan balance having accuracy upto 0.0001 gms.

The mechanical mixing of Lead powder, containing different dispersoids separately was carried out by manual mixing. The operational details about the mixing are given in Table 2.1. The compositions of different composites both in weight and volume percentages are summarised in Table 2.2.

2.2.2 Compaction

Unidirectional compaction at room temperature was carried out on a Riehle compression testing machine (capacity 135000 kg). The compaction die was made up of En-8 Steel of diameter 42 mm and height 60 mm with the wall thickness 50 mm. Zinc stearate was used as the die lubricant. The details about the compaction pressures are summarised for various processes in Table 2.1.

2.2.3 Sintering

The compacted green pellets (40 mm dia x 25 mm height approximately) of the composites were sealed in evacuated pyrex tubes. The vacuum maintained was 10^{-3} torr for all the composites. These evacuated and sealed tubes were heated for sintering at 280°C (0.92 T_m) in a horizontal tubular furnace where a constant temperature zone of 100 mm was maintained.

2.2.4 Extrusion

The room temperature extrusion was carried out on the same compression testing machine mentioned earlier. Die used for the extrusion was made up of air-hardening high carbon-high chromium steel. The die angle was 60° with an outlet diameter of 10.4 mm. The extrusion ratio and speed of extrusion were maintained to be 16:1 and 1 cm/min respectively throughout this study. Zinc stearate was used as die lubricant during extrusion.

2.2.5 Swaging

The extruded rod of 10.4 mm diameter was further swaged in one of the processes adopted for development of these Lead base composites at room temperature. The details about the swaging are incorporated in Table 2.1.

The different combinations of the above-mentioned techniques were done in order to develop various processes and to assess their effects on mechanical properties of the

composites. Such processes used in preparing composites are designated as Process I, Process II, Process III and Process IV. The appropriate details of these processes are summarised in Table 2.1.

2.2.6 Annealing treatments

The composites thus prepared were given final annealing treatments, the details of which, are also incorporated in Table 2.1.

2.3 Porosity Measurements

Porosity measurements were done at various stages of the processing routes of different composites. Porosity was calculated by formula:

$$\% \text{ Porosity} = 100 - \% \text{ relative density} \qquad (2.1)$$

where relative density was determined by the ratio of observed density to the theoretical density. The density of green compacts (40 mm dia (D) and 26 mm height (H) approximately) and cylindrical machined samples of 10 mm diameter (d) and 7 mm height (h) was determined by physical dimension measurements and checked for certain samples by displacement method. The volume measurement in first method was done through dimensional method, where $V = \dfrac{\pi\, d^2 \times h}{4}$, whereas displacement method was used in the latter case.

2.4 Microstructural Examination:

Microstructural characterisation of Lead-base particulate composites prepared through Processes III and IV was done through grain size measurements (Intercept method), grain aspect ratio (GAR), particle-distribution of dispersoids by means of optical microscope. The specimens were examined both in transverse and longitudinal directions with respect to extrusion axis.

Lead is a soft metal which is difficult to polish mechanically. To avoid mechanical polishing during metallographic specimen preparation, smooth surface was obtained directly by machining the flat surface of the sample on a lathe. This was followed by chemical polishing[55] in a solution consisting of 50 cc glacial acetic acid, 30-50 cc H_2O_2 (30% H_2O_2) and 1-2 cc concentrated nitric acid. The chemical polishing was carried out by dipping the specimens in the polishing solution for 5 to 6 seconds. After chemical polishing, etching was carried out with a reagent consisting of ammonium molybdate (10 gms), citric acid (25 gms) and water (100 cc). The etching time was about 5 to 15 seconds.

2.5 Mechanical Testing:

Mechanical tests, namely, tension, compression and creep were conducted to evaluate mechanical behaviour of Lead-base particulate composites. The compression and tension tests were carried out on Instron machine of 5000 kg capacity.

2.5.1   Compression tests

Compression test was carried out on the longitudinal section of the cylindrical specimens (Figure 2.1) having L/D ratio, where L and D were length and diameter of the specimen in mm, of 1.5. Cylindrical specimens of (i) 5.1 mm diameter and 7.65 mm length and (ii) 6 mm diameter and 9 mm length were used for compression tests, in order to get strain rate comparable to tension test (3.7×10^{-4} $\sec^{-1}$).

Transverse compression having specimen axis perpendicular to the extruded rod axis was carried out on the specimens (Figure 2.1) where L/D ratio was 1.5. The specimen dimensions were similar to (i) of longitudinal compression specimen mentioned earlier.

Longitudinal compression tests were conducted at 3.7×10^{-4} $\sec^{-1}$ and 2.2×10^{-4} $\sec^{-1}$ strain rates, while transverse compression test was conducted at 2.2×10^{-4} $\sec^{-1}$ strain rate only. All compression tests were done at room temperature (28°C) only.

2.5.2   Tension test

The specimen dimensions used for tension test are shown in Figure 2.1. The specimens were prepared out of the extruded/annealed   rods where longitudinal axis of the specimen was parallel to the extruded rod axis. Tensile tests, at constant cross head speed were conducted in silicone oil bath

from 0.51 to 0.76 T_m temperature range. The selected strain rate was 3.7×10^{-4} sec^{-1}. The holding time at any particular temperature was 30 minutes prior to actual testing.

2.5.3 Creep test

Constant stress creep tests were performed using a double shear specimen[59] (Figure 2.1). The advantage of a double shear specimen is that constant stress is maintained on a sample at constant load since the area of the specimen remains constant with shear strain.

2.5.3.1 Sample fixtures and creep testing machine

For holding shear specimen, special split grips in three parts as shown in Figure 2.2, were prepared out of 70:30 brass. The central portion of the specimen was fixed in the middle split grip, while two ends of the specimen were fitted in the other two split grips which were in turn rigidly fixed on the bottom plate of the cage made up of En-8 steel.

The sample was loaded through the lever arm (lever ratio 20:1) by means of standard weight kept on the bale pan (Figure 2.3). Before starting the creep tests, the lever arm was carefully balanced through the adjustable counter-weight which is provided on the lever arm of the creep machine.

2.5.3.2 Measuring and recording of strain

The displacement measuring system consisted of a Linear Variable Differential Transformer (LVDT). The function of LVDT is to convert the supplied mechanical displacement into electronic signal as its output. This output through an Amplifier is fed to the recorder (Brown-Strip Chart recorder) for recording it continuously. The sensitivity of displacement measuring system is 2.5×10^{-3} mm. The details of positioning of LVDT are shown in Figure 2.4.

2.5.3.3 Calibration of LVDT

A small knurled knob connected to a worm and wheel arrangement provides a fine mechanical adjustment of transformer core position for zeroing. After zeroing the transformer core position, filler gauges of various sizes were inserted in between the knurled knob and transformer core so as to give the mechanical displacement to the measuring unit. It is ensured that the 0.5 mm thick gauge, i.e. 0.5 mm mechanical displacement of the transformer core in "HI" range of the recorder, mentioned earlier, corresponds to full scale deflection of the recorder pen. The above procedure was used to check the calibration of the displacement measuring system before the start of each creep test.

2.5.3.4 Temperature control system

The test temperatures were attained by means of a silicone oil bath heated electrically and the temperature of the oil bath was controlled through an appropriate controller within $\pm 2°C$.

2.5.3.5 Test details

The creep tests were carried out in shear stress range of 1 to 11 MPa. The test temperatures were selected to be 100°C, 150°C and 180°C. The holding time of the specimen for stabilisation of the temperature was a minimum of 15 hrs prior to actual start of the test. Creep tests were conducted upto 96 hrs depending upon the applied stress and temperature. The creep tests were terminated after either zero, creep rate or steady state creep rate was attained.

2.5.3.6 Internal stress measurements

The internal stress measurements were done in the steady state creep region. Having attained steady state rate at a given stress level, small stress reductions ($\Delta \tau$) of 0.1 τ_A, where τ_A is the applied shear stress, were made. After recording the creep strain for sometime following the stress reduction, a further reduction in stress of 0.1 τ_A was made and this procedure was repeated till a negative creep rate was observed. The shear stress corresponding to zero creep rate in such a test was taken as the internal stress (τ_i) for the applied shear stress and temperature.

Table 2.1

Techniques used for processing Lead-base composites

Technique	Process I	Process II	Process III	Process IV
Manual mixing (hr)	0.25	0.25	1.00	1.00
Compaction pressure (MPa)	128.00	128.00	128.00	384.00
Sintering				
Temperature ($^\circ$C)	Nil	Nil	280.00	280.00
Period (hrs)	Nil	Nil	100.00	100.00
Extrusion (extrusion ratio)	16:1	16:1	16:1	16:1
Swaging (% reduction in area)	Nil	64.00	Nil	Nil
Final annealing				
Temperature ($^\circ$C)	200	200	280	280
Period (hrs)	3.50	1.50	2.00	2.00 and 100.00

Table 2.2

Compositions of Lead-base particulate composites

Composite	Dispersoids in wt. %			Dispersoids in vol. %		
	PbO	Zn	Al_2O_3	PbO	Zn	Al_2O_3
P/M Lead	1.00	-	-	2.50	-	-
Pb-Zn	1.00	1.86	-	2.50	2.50	-
	1.00	3.73	-	2.50	5.00	-
	1.00	5.60	-	2.50	7.50	-
Pb-Al_2O_3	1.00	-	0.87	2.50	-	2.50
	1.00	-	1.73	2.50	-	5.00
	1.00	-	2.60	2.50	-	7.50

(b) Tension test specimen.

(a) Longitudinal compression test specimen.

(d) Creep test specimen.
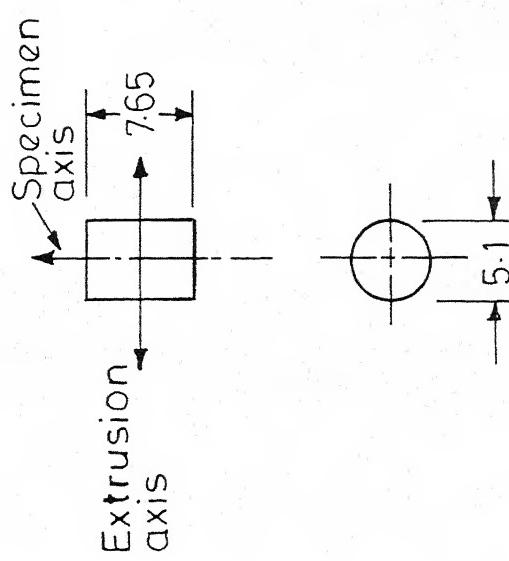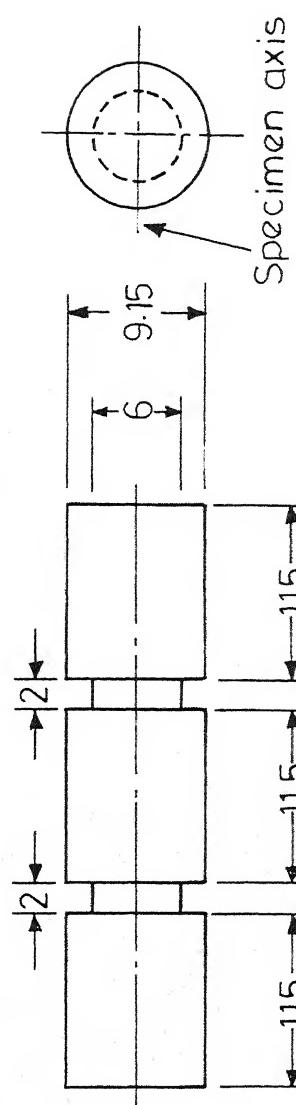
(c) Transverse compression test specimen.

All dimensions in mm.

Fig. 2.1 – Various test specimens.

Creep specimen
(double shear)
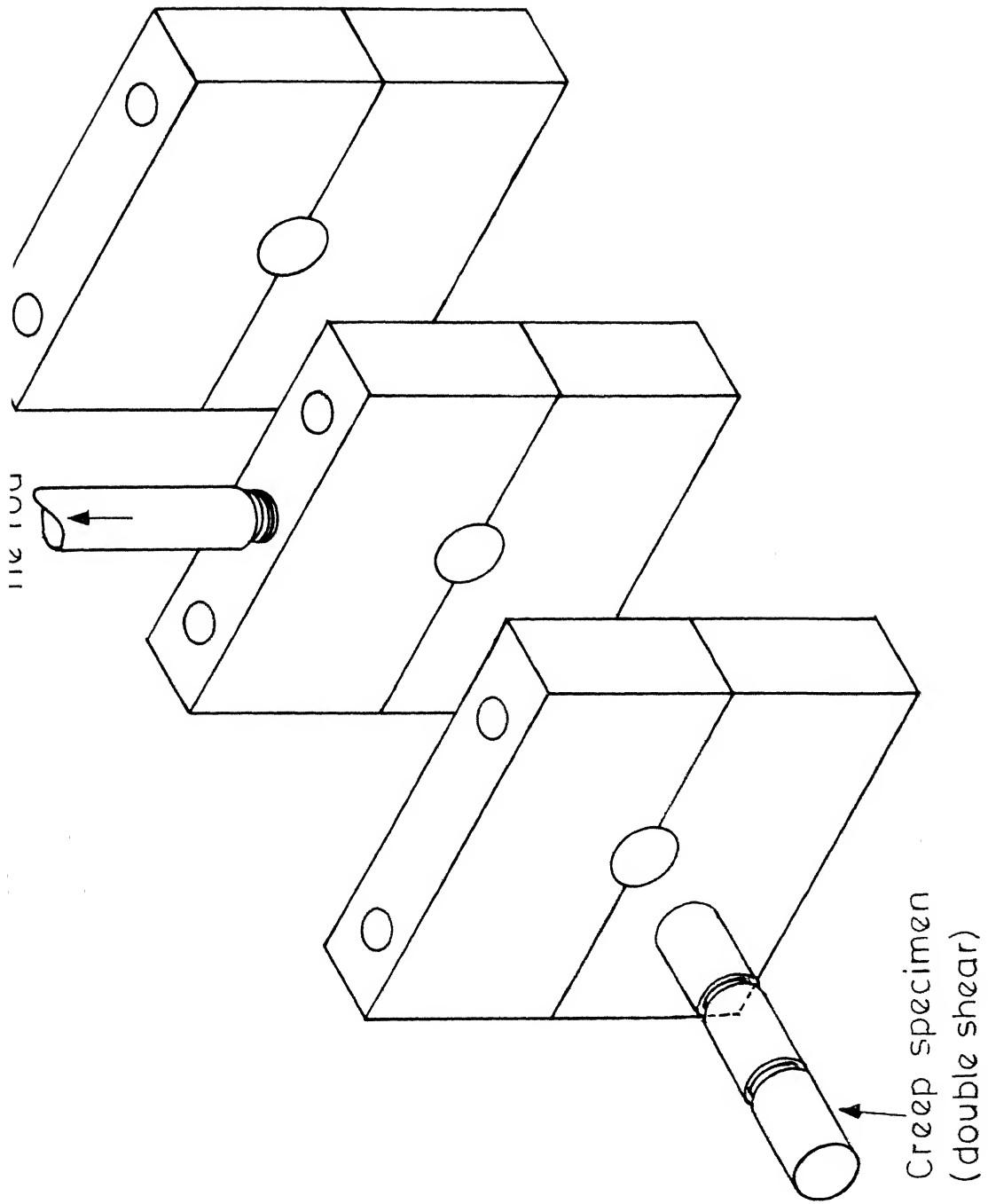
Fig. 2.2 - Grips for double shear specimen.

1. Screw jack
2. Cage
3. Specimen grips
4. Temperature bath
5. Specimen
6. Cage supporting plate
7. LVDT
8. Extension rod
9. Strain recorder
10. Load
11. Controller
12. Supporting frame
13. Counter wt.
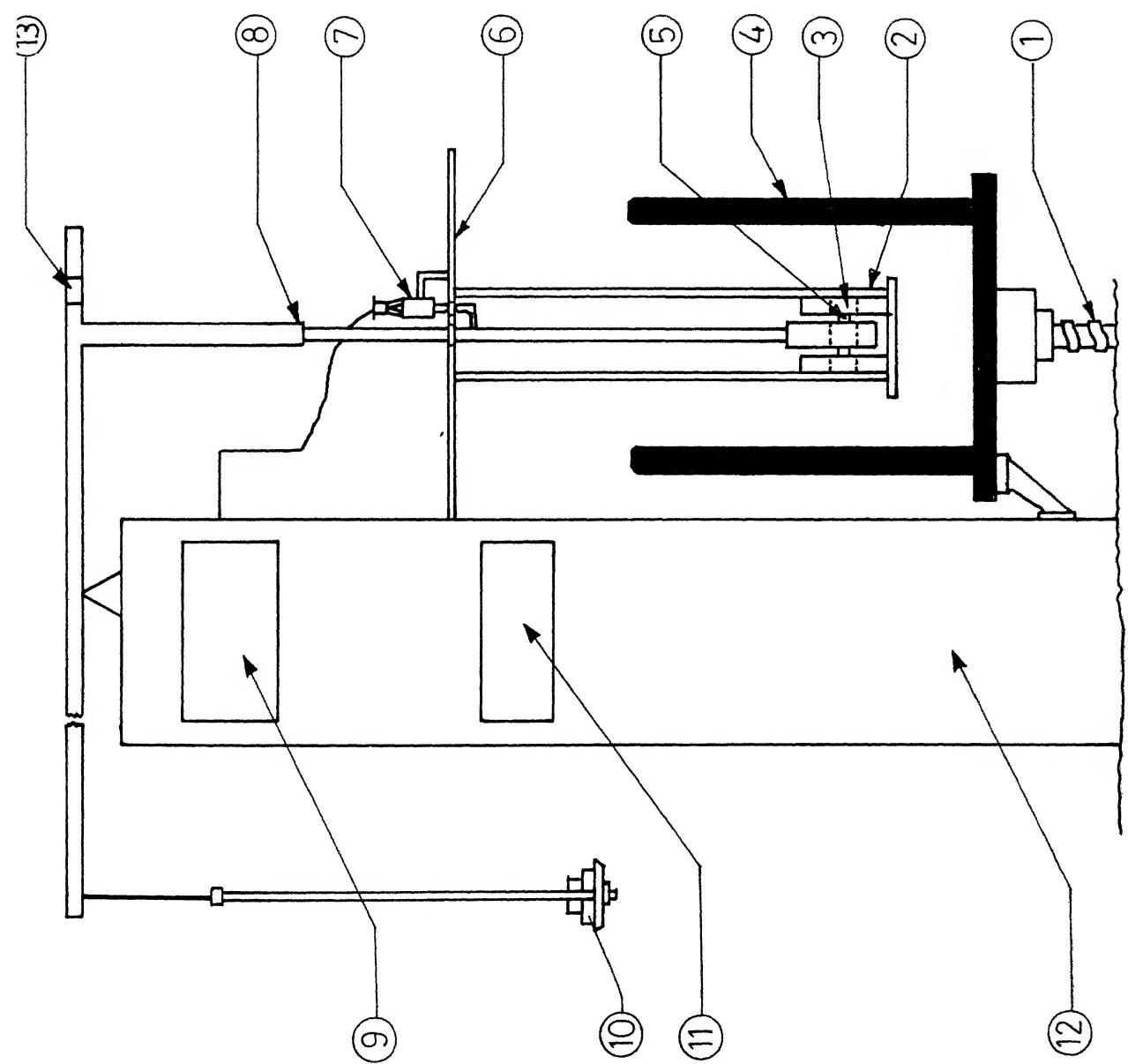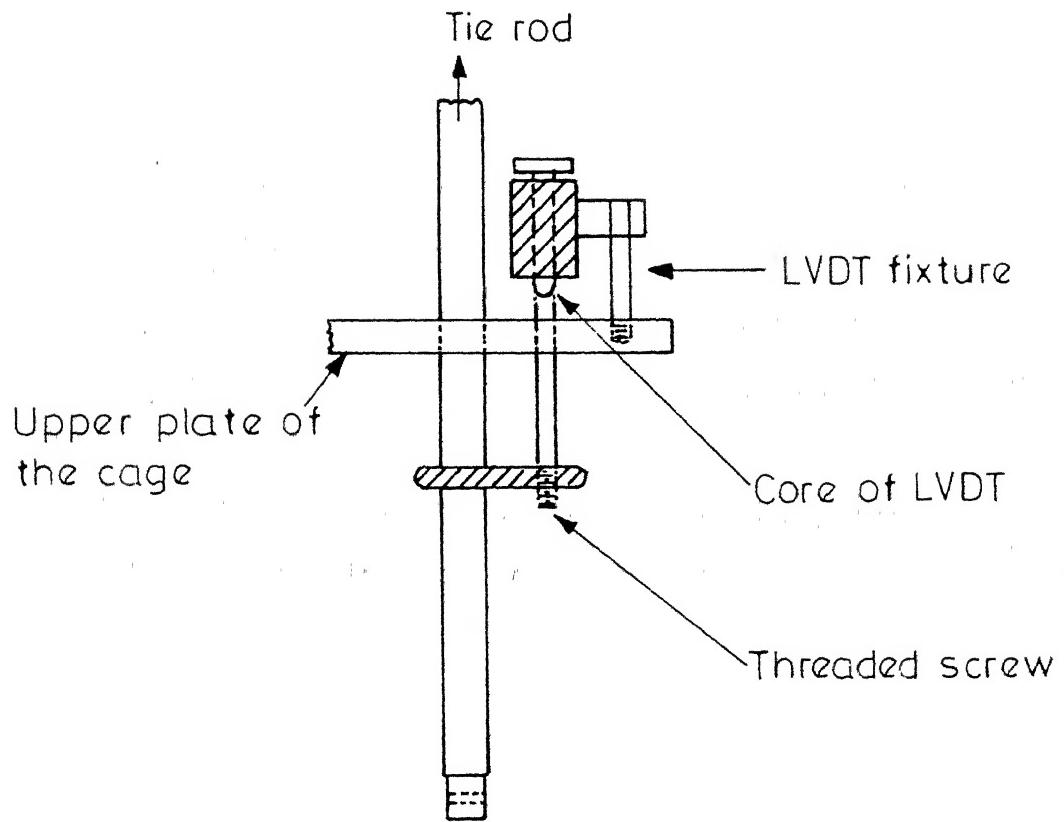
Fig. 2.4 – LVDT assembly along with tie rod.

CHAPTER III

EXPERIMENTAL RESULTS

The results of the present investigation are presented
in this chapter. The effects of processing variables on the
characteristics of Lead-base P/M particulate composites, prepared
through four different processes as described in earlier
Chapter II, are summarised in Section 3.1. The characterisation
was done on the basis of porosity, extrusion pressure, compressive
yield strength and SD effect. In Section 3.2, the results of
the mechanical behaviour of the composites prepared through
Process IV are reported. The mechanical behaviour that has
been investigated consists of SD effect, tensile and creep tests
at various temperatures.

3.1 Effect of Processing Variables on the Characteristics of Lead-base-Composites

3.1.1 Porosity

The porosity measurements were carried out at every
stage of processing, namely, compaction, extrusion, swaging
and annealing depending upon the process followed. The
porosity data of Lead-base composites prepared through four
different processes are summarised in Tables 3.1, 3.2, 3.3

and 3.4 for respective processes. Further, the combined statement of final porosity is given in Table 3.5.

These porosity data given in Table 3.5 clearly indicate that the porosity level in a composite of a given composition depends upon the process adopted. The decreasing trend in porosity is observed from Process I to IV. Further, in composites of Process IV, the porosity levels increased with the volume content of the dispersoid. It may also be noted that under identical processing conditions porosity level varies depending on the nature of the dispersoid. Further, it is noticed that the annealing after extrusion in all the four processes has insignificant effect in further reducing the porosity level of the composites (Tables 3.1 to 3.4).

3.1.2 Extrusion pressure

pressure
The extrusion/data presented in Table 3.6 shows that the extrusion pressure increases from Process I to IV. The increase in extrusion pressure is insignificant from Process I to III for all the composites. However, in Process IV, the extrusion pressure values have increased substantially for P/M Lead and $Pb-Al_2O_3$ composites.

The magnitude of extrusion pressure was observed to depend on the nature of the dispersoid. Under identical processing conditions, $Pb-Al_2O_3$ composites have always shown higher values than that of the Pb-Zn composites. Further, the effect of the dispersoid volume content effect on the

extent of extrusion pressure is illustrated in Figure 3.1. $Pb-Al_2O_3$ composites have shown increasing trend in extrusion pressure with dispersoid volume content. On the other hand, a decreasing trend in extrusion pressure was observed with the addition of Zinc dispersoid in Lead base composites.

3.1.3 Microstructural observations

Microstructural observations both in longitudinal and transverse directions to the extrusion axis are made on P/M Lead, Pb-5 V/O Zn and Pb-5 V/O Al_2O_3 composites prepared through Processes III and IV only because the composites obtained from Processes I and II have shown more variation in microstructural homogeneity and fibering effect in addition to the variation in density and compressive strength in comparison to composites prepared through Processes III and IV. Some typical transverse photomicrographs are shown in Figures 3.2 and 3.3. Figure 3.2 represents the microstructure of composites prepared through Process III and annealed for 2 hrs at 280°C while Figure 3.3 refers to the microstructure of composites prepared out of Process IV followed by annealing at 280°C for 100 hrs.

In the composites prepared by Process III, the dispersoids are observed to be predominantly at the grain boundaries as shown in Figure 3.2. Similar distribution of dispersoids is observed in Lead-Zinc composites of Process IV. However, in case of P/M Lead and $Pb-Al_2O_3$ composites of

Process IV, the dispersoids are observed to be at grain boundaries as well as within the grains to some extent.

The transverse grain size values are reported for these composites in Table 3.7. Further, the composites prepared through Process III (2 hrs annealed at 280°C), Process IV (as extruded) and Process IV followed by 2 hrs annealing at 280°C have exhibited elongated grains in the direction of extrusion with an approximate grain aspect ratio (GAR) of 1.2, whereas, in all the composites of Process IV followed by 100 hrs annealing at 280°C, GAR was found to be below 1.1.

3.1.4 Compressive yield strength

The longitudinal compressive yield strength values of Lead-base composites prepared through various processes are summarised in Table 3.8.

The results show that the compressive yield strength values are improved from process to process except in case of $Pb-Al_2O_3$ for Process IV. There is a larger increase in yield strengths for P/M Lead and $Pb-5$ v/o Zn in comparison to $Pb-5$ v/o Al_2O_3.

The results obtained so far for porosity, extrusion pressure and compressive yield strength indicate that the composites prepared through Processes I and II are inferior to those prepared through Processes III and IV in terms of density, compressive strength and microstructural homogeneity.

Hence, rest of the investigations are carried out on composites prepared by Processes III and IV only. Having discontinued the studies on composites prepared through Processes I and II, the further characterisation of the composites prepared by Processes III and IV is carried out by studying the anisotropy in compressive strength and SD effect.

The compressive yield strength values in transverse and longitudinal direction for the composites annealed for 2 hrs after preparing by Processes III and IV as well as composites of Process IV (as extruded) are reported in Table 3.9.

It is observed that yield strength values in transverse direction are always greater than those in longitudinal direction (anisotropic effect) in all the composites irrespective of the processing route followed for the preparation of these composites. Moreover, it may be noted that in a particular process, the magnitude of anisotropic effect is decreasing from Pb-5 v/o Zn, Pb-5 v/o Al_2O_3 to P/M Lead composites.

3.1.5 Strength differential (SD) effect

The stress-strain curves in tension and compression for Lead-base composites at room temperature are presented for Processes III and IV in Figures 3.4 and 3.5 respectively. It was observed that the compression and tension yield strength values were different in materials by either of the

above two processes. The results in Figure 3.4 indicate
that all the composites of Process III have shown higher
yield values in compression than in tension. The observed
SD effect between tension and compression values was in
decreasing order from Pb-5 V/o Zn, P/M Lead to Pb-5 V/o Al_2O_3.
The results on composites prepared by Process IV indicate
(Figure 3.5) a completely different trend in SD effect than
that is seen in Process III, while Pb-5 V/o Zn has exhibited
positive SD effect, Pb-5 V/o Al_2O_3 and P/M Lead composites
showed a negative SD effect, i.e., tensile yield strength
values were greater than those in compression. The processing
history has thus modified the extent and sign of the SD effect.

The anisotropy in compressive strength is observed
to be less in composites of Process IV in comparison to
Process III. It may also be noted from the above observations
on SD effect that the composites prepared through Process IV
are superior in terms of their tensile strength to those
prepared by Process III and hence, further, evaluation of
mechanical behaviour was carried out on the composites
prepared through Process IV only.

3.2 Mechanical Behaviour of Composites Prepared Through Process IV

3.2.1 Variation of SD effect with dispersoid volume content

The variation of SD effect with volume content of
dispersoid as well as state of the composites, namely, as

extruded and annealed (280°C for 2 hrs), is summarised in Table 3.10. These composites have exhibited increasing trend in SD with increasing dispersoid volume content for Pb-Zn. However, in case of Pb-Al_2O_3 composites, SD is negative and changes marginally with the dispersoid volume content.

It is apparent from Table 3.10 that all the composites in as extruded condition show smaller SD effect in comparison to the annealed composites. Further, it is revealed that SD effect depends upon the nature of dispersoid. Zinc containing composites have exhibited positive SD effect while negative SD effect is shown by Pb-Al_2O_3 composites.

In view of the fact that the quality of P/M products can better be assessed by tensile test rather than compression test, the further studies are confined to tensile testing only.

3.2.2 Effect of temperature on tensile properties

The 0.2% offset yield strength values at room temperature (28°C), 100°C and 180°C are presented in Table 3.11. Some typical stress-strain plots are shown in Figures 3.6 to 3.9.

It is revealed from these results that the yield strength of Pb-Al_2O_3 composites is maximum at all temperatures irrespective of the state of the composites. Composites in as extruded condition exhibit higher yield strength as compared to those of 100 hrs annealed composites. The same

trend is maintained at all the temperatures (Figure 3.10).
Further, the yield strength of all the composites decreases
with increasing temperature (Figures 3.11 and 3.12).

Pb-Zn composites have shown lower yield strength
values than those of P/M Lead. All the composites show better
strength than pure Lead prepared through conventional route
(melting-casting-extrusion) over all the temperature range
studied.

3.2.3 Effect of volume fraction on tensile properties

The yield strength of the composite depends upon
the dispersoid volume content as shown in Figures 3.13 and
3.14. This property is marginally improved over P/M Lead
with dispersoid content in case of $Pb-Al_2O_3$ composites, both
in as extruded and 100 hrs annealed conditions. However,
Pb-Zn composites showed decreasing trend with respect to.P/M
Lead in yield strength value for the studied dispersoid volume
fractions in both the states mentioned earlier. It is revealed
from these results that dispersoid nature is an influential
factor in yield strength values of the composites. $Pb-Al_2O_3$
composites have shown higher values over to P/M Lead, while
Pb-Zn composites have exhibited lower values with respect to
P/M Lead.

3.2.4 Ductility of Lead-base composites

Ductility vs. dispersoid volume percentage plots
obtained from the tensile tests are given in Figure 3.15.

These plots show the variation of the ductility with respect to both the volume content and temperature for Lead-base composites in as extruded and 100 hrs annealed condition.

It is observed that the ductility decreases with the volume content irrespective of the type of dispersoid. In as extruded condition, the Pb-Zn composites have shown moderately higher ductility values than those of Pb-Al_2O_3 for a particular temperature. Further, in all the composites ductility values decrease with temperature.

In comparison to ductility values in as extruded state, 100 hrs annealed Lead-base composites have shown substantial improvement in ductility (Figure 3.15). Decreasing trend in ductility with respect to volume fraction obtained in 100 hrs annealed composites is similar to that obtained in as extruded state.

3.2.5 Creep behaviour

Creep data have been collected for P/M Lead, Pb-5 v/o Zn and Pb-5 v/o Al_2O_3 composites (2 hrs annealed) at 100°C, 150°C and 180°C in shear stress range of 1 to 11 MPa. Typical creep curves are shown in Figure 3.16 for 100°C the applied shear stresses below 6 MPa depending upon the composite. The instantaneous creep strain vs. applied shear stress plots are presented in Figure 3.17 for 100°C, 150°C and 180°C. A linear relationship was observed between instantaneous strain and applied shear stress for these

composites at all the tested temperatures. For a given stress, instantaneous strain increases with increasing temperature. Further, for a particular stress and temperature, maximum instantaneous strain was shown by Pb-5 V/O Zn and minimum by Pb-Al$_2$O$_3$ composites. Pb-5 V/O Zn has shown higher instantaneous strain than that for P/M Lead (Figure 3.17). In case of P/M Lead and Pb-5 V/O Al$_2$O$_3$ composites, creep rate continuously decreased with strain at low stresses upto 100°C (Figure 3.16). This behaviour was absent for Pb-5 V/O Zn composites.

The stress dependence of steady state shear creep rate, $\dot{\gamma}_s$, observed in Lead-base composites at 100°C, 150°C and 180°C is shown in Figure 3.18. From this figure, it can be noted that these composites have different stress exponents (n_a) in different regions (i.e. low and high stress exponent regions). The apparent stress exponents (n_a) for Pb-Zn composites are 2.8 and 7.5 at low and high stress exponent regions respectively. However, three distinct regions were obtained for P/M Lead, Pb-5 V/O Al$_2$O$_3$ at 100°C and 150°C. Below 150°C, for these composites threshold stresses are observed (Figure 3.18) where, $\dot{\gamma}_s$, is zero. The apparent stress exponents (n_a) in the steady state, $\dot{\gamma}_s$, regions for P/M Lead and Pb-Al$_2$O$_3$ for two regions are summarised in Table 3.12.

From the Figure 3.18, it is evident that the change in apparent stress exponent occurred at 10^{-6} sec^{-1} shear strain rate in all the cases. However, the corresponding

stress levels were different depending on the composite.
Further, n_a was observed to be independent of temperature in
all cases (Table 3.12). These results are indicative of the
fact that **the** dispersoid nature has an effect on the n_a values
of these composites.

Internal stress measurements were carried out on P/M
Lead at 150°C. Figure 3.19 shows the measured relationship
between τ_a (applied shear stress) and τ_i (measured internal
shear stress). Here, τ_a was in the range of 2 to 8.5 MPa.
The plot of log $\dot{\gamma}_s$ vs. log τ_e (τ_e = effective shear stress =
$\tau_a - \tau_i$) is also incorporated in Figure 3.18. This log $\dot{\gamma}_s$ vs.
log τ_e plot for P/M Lead indicate two regions of different
stress exponents n_e, where n_e is effective stress exponent. Effec-
tive stress exponents (n_e) are 1.0 and 5.2 for these two
regions.

The temperature dependence of steady state, $\dot{\gamma}_s$, is
illustrated in Figure 3.20 for low and high n_a regions. The
apparent activation energies (Q_a) for these composites in low
and high stress exponent regions are summarised in Table 3.13.

It is apparent from Q_a values given in Table 3.13
that these values for all these composites over low stress
exponent region are lower than the self diffusion activation
energy (Q_{SD}), which is 22.92 kcal/mol [60] for Lead. On the
other hand, in high stress exponent region, Q_a values are
closer to Q_{SD} for Lead. Further, it is observed that Q_a

values for both P/M Lead and Pb-5 v/o Al_2O_3 composites are higher than Pb-5 v/o Zn composites irrespective of the stress and temperature of testing.

Table 3.1

Composite processing – Process I

Composite	Room temperature compaction		Room temperature extrusion		Final annealing (200°C)
	Compaction pressure (128 MPa)		Extrusion ratio (16:1)		Duration (3.50 hrs)
	Green density (gm/cc)	Porosity in %	Extrusion pressure (MPa)	Porosity in %	Porosity in %
P/M Lead	8.36	25.30	207.00	9.80	9.70
Pb·.5 v/o Zn	8.12	27.60	228.00	10.70	10.60
Pb–5 v/o Al_2O_3	8.06	28.60	240.00	13.00	12.60

Note: Variation in porosity from lot to lot is around 4%.

Table 3.2

Composite processing - Process II

Composite	Room temperature compaction		Room temperature extrusion		Swaging (room temperature)	Final annealing (200°C)
	Compaction pressure (128 MPa)		Extrusion ratio (16:1)		Reduction in area (64%)	Duration (1.5 hrs)
	Green density (gm/cc)	Porosity in %	Extrusion pressure (MPa)	Porosity in %	Porosity in %	Porosity in %
P/M Lead					2.70	2.60
Pb-5 v/o Zn	Same as Process I		Same as Process I		3.20	3.10
Pb-5 v/o Al_2O_3					4.40	4.35

Table 3.3

Composite processing – Process III

Composite	Room temperature compaction		Vacuum sintering (10^{-3} Torr) at 280°C	Room temperature extrusion		Final annealing (280°C)
	Compaction pressure (128 MPa)		Duration (100 hrs)	Extrusion ratio (16:1)		Duration (2 hrs)
	Green density (gm/cc)	Porosity in %	Porosity in %	Extrusion pressure (MPa)	Porosity in %	Porosity in %
P/M Lead			7.0	215.0	0.4	0.4
Pb-5 v/o Zn	Same as Process I		9.6	222.0	0.8	0.7
Pb-5 v/o Al_2O_3			10.5	245.0	1.2	1.1

Note: The porosity variation in as sintered compacts is observed to be 2%.

Table 3.4

Composite processing - Process IV

Composite	Room temperature compaction (28°C)		Vacuum sintering (10⁻³ Torr) at 280°C	Room temperature extrusion (28°C)		Final annealing (280°C)
	Compaction pressure (384 MPa)		Duration (100 hrs)	Extrusion ratio (16:1)		Duration (2 hrs & 100 hrs)
	Green density ( )	Porosity in %	Porosity in %	Extrusion pressure (MPa)	Porosity in %	Porosity in %
P/M Lead	98.7	1.3	0.8	250	0.2	0.1
Pb-						
2.5 v/o Zn	93.0	2.0	1.6	240	0.4	0.1
5 v/o Zn	96.0	4.0	2.8	230	0.6	0.4
7.5 v/o Zn	93.5	6.5	4.6	215	1.4	1.2
Pb-						
2.5 v/o Al_2O_3	96.5	3.5	2.6	260	0.7	0.6
5 v/o Al_2O_3	94.7	5.3	3.7	275	1.2	1.0
7.5 v/o Al_2O_3	92.5	7.5	5.0	291	2.2	1.6

Table 3.5

Final % porosity data of Lead-base particulate
composites (Processes I-IV)

Composite	Process I	Process II	Process III	Process IV
P/M Lead	9.70	2.60	0.40	0.10
Pb-5 v/o Zn	10.60	3.10	0.70	0.40
Pb-5 v/o Al$_2$O$_3$	12.90	4.35	1.10	1.00

Table 3.6

Extrusion pressures (MPa) of Lead-base particulate
composites (Processes I-IV)

Composite	Process I	Process II	Process III	Process IV
P/M Lead	207	207	215	250
Pb-5 v/o Zn	228	228	222	230
Pb-5 v/o Al$_2$O$_3$	240	240	245	275

Table 3.7

Transverse grain size values for Lead-base
particulate composites (Processes III & IV)

Process	Transverse grain size μm		
	P/M Lead	Pb-5 v/o Zn	Pb-5 v/o Al$_2$O$_3$
Process III Annealed at 280°C for 2 hrs	10.0	12.0	9.5
Process IV a) As extruded	8.0	10.0	8.0
b) Annealed at 280°C for 2 hrs	9.0	12.5	9.0
c) Annealed at 280°C for 100 hrs	17.0	30.0	16.0

Note: Grain sizes obtained after 2 hrs annealing at 280°C
in Pb-7.5 v/o Zn and Pb-7.5 v/o Al$_2$O$_3$ are 19 and 10
μm respectively.

Table 3.8

Longitudinal compressive yield strength (MPa) values
of Lead-base composites (Processes I-IV)

Composite	Process I	Process II	Process III	Process IV
P/M Lead	14.5	17.0	20.8	21.2
Pb-5 V/O Zn	17.0	20.7	21.6	22.4
Pb-5 V/O Al_2O_3	22.6	23.4	24.6	22.6

Note: The variation in compressive strength values are
observed to be 4%, 3.5%, 2% and 1.6% for Processes I,
II, III and IV respectively.

Table 3.9

Anisotropic effects in Lead base composites prepared by Processes III and IV

Composite	Process III			Process IV					
	2 hrs annealed (280°C)			2 hrs annealed (280°C)			As extruded		
	σ_{CT}	σ_{CL}	Aniso-tropy in %	σ_{CT}	σ_{CL}	Aniso-tropy in %	σ_{CT}	σ_{CL}	Aniso-tropy in %
P/M Lead	21.4	20.8	3.0	21.4	21.2	1.0	20.2	19.2	5.4
Pb-5 v/o Zn	25.8	21.6	17.0	24.5	22.4	8.8	26.0	22.6	13.0
Pb-5 v/o Al$_2$O$_3$	25.6	24.6	4.0	23.8	22.6	5.1	24.6	23.0	65

Note: % Anisotropy $= \dfrac{\sigma_{CT} - \sigma_{CL}}{\sigma_{CT}} \times 100$

where σ_{CT} - compressive yield in transverse direction to extrusion axis

σ_{CL} - compressive yield in longitudinal direction to extrusion axis.

Net SD effect in Lead-base particulate composites (Processes III & IV

Process	Observation	P/M Lead	Pb-Zn			Pb-Al$_2$O$_3$		
			2.5	5.0	7.5	2.5	5.0	7.5
III (annealed at 280°C, 2 hrs)	observed SD effect	+7.0		+24.0			+13.0	
	SD effect due to porosity *	+1.0		+ 2.8			+ 4.5	
	Net SD effect	+6.0		+21.2			+ 8.5	
IV (as extruded)	observed SD effect	-3.0	-2.0	+11.0	+15.0	-5.0	- 7.0	- 6.0
	SD effect due to porosity	+1.6	+2.5	+ 3.2	+ 5.8	+3.6	+ 5.2	+ 7.7
	Net SD effect	-4.6	-4.5	+ 7.8	+ 9.2	-8.6	-12.2	-13.7
IV (annealed at 280°C, 2 hrs)	observed SD effect	-2.0	+7.0	+12.2	+18.0	-3.0	- 5.0	- 4.0
	SD effect due to porosity	+1.0	+1.2	+ 2.5	+ 5.2	+3.2	+ 4.6	+ 6.2
	Net SD effect	-3.0	+5.8	+ 9.7	+12.8	-6.2	- 9.6	-10.2

Note: SD effect is represented in the following manner:

$$\% \ SD = \frac{\sigma^C_{0.2\%} - \sigma^T_{0.2\%}}{\sigma^C_{0.2\%}} \times 100$$

where $\sigma^C_{0.2\%}$ and $\sigma^T_{0.2\%}$ are 0.2% offset yield strength values in compression and tension respectively.

* Refer page 87.

Table 3.11

Tensile yield strength (MPa) values of Lead-base particulate composites (Process IV)

Material	Room temperature (28°C)		100°C		180°C	
	As extruded	100 hrs annealed	As extruded	100 hrs annealed	As extruded	100 hrs annealed
Pure Lead	10.8	8.6	4.8	6.3*	3.6	4.0
P/M Lead	21.2	16.0	15.8	14.0	9.0	8.0
Pb-5 V/O Zn	18.8	14.0	11.2	10.8	8.0	7.0
Pb-5 V/O Al_2O_3	22.0	18.6	17.7	15.8	10.4	10.0

* Value estimated from the graph in Figure 3.12.

Table 3.12

Apparent stress exponents (n_a) for Lead-base components
(Process IV)

Composite	Low stress region			High stress region		
	Temperature °C			Temperature °C		
	100	150	180	100	150	180
P/M Lead	3.0	3.0	3.0	10.0	10.0	10.0
Pb-5 V/O Zn	2.8	2.8	2.8	7.5	7.5	7.5
Pb-5 V/O Al$_2$O$_3$	3.5	3.5	3.5	12.0	12.0	12.0

Table 3.13

Q_a and n_a for Lead-base composites
(Process IV)

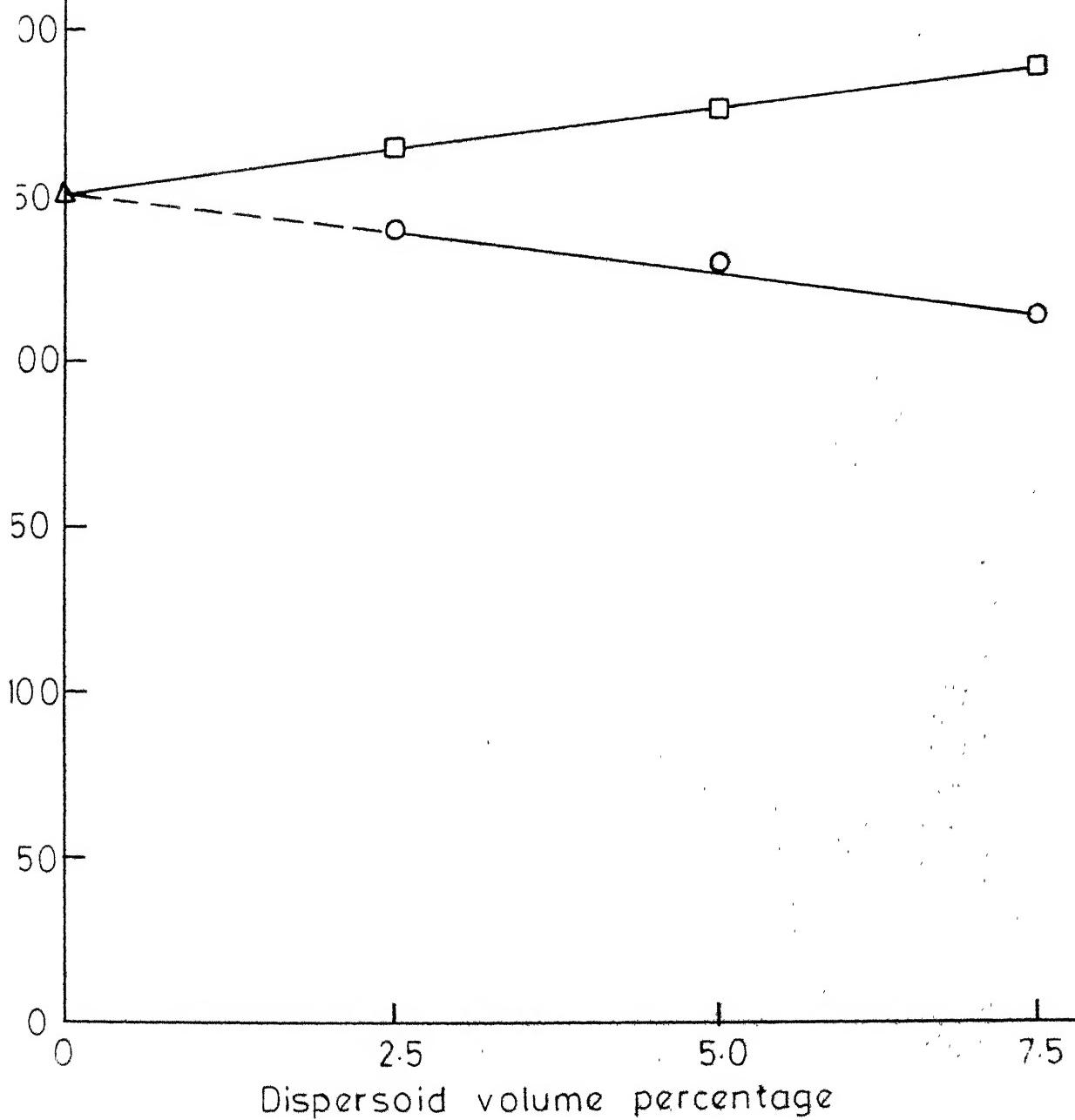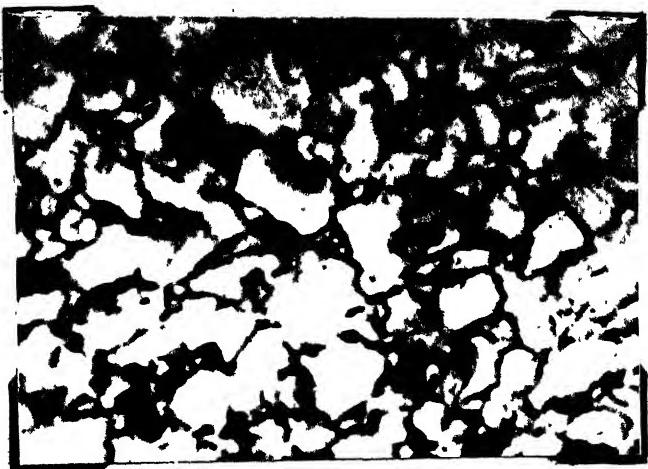| Composite	P/M Lead		Pb-5 V/O Zn		Pb-5 V/O Al$_2$O$_3$	
	Low stress exponent region	High stress exponent region	Low stress exponent region	High stress exponent region	Low stress exponent region	High stress exponent region
n_a	3.00	10.00	2.80	7.50	3.50	12.00
Q_a (kcal/mol)	9.25	30.00	7.20	20.70	10.40	33.00

Fig. 3·1 – Effect of dispersoid volume fraction on extrusion pressure at room temperature.

(a) P/M Lead

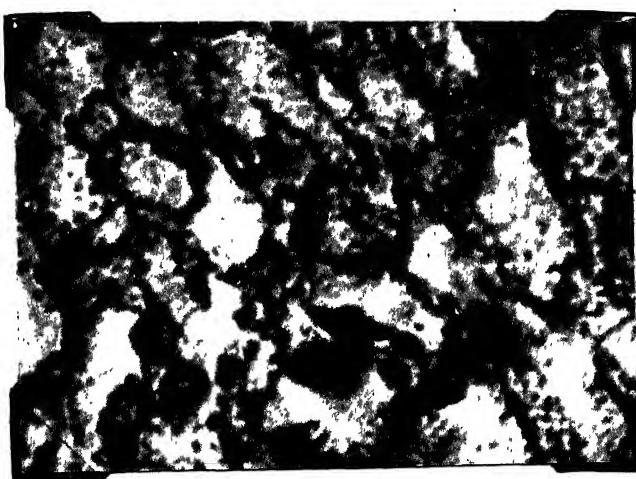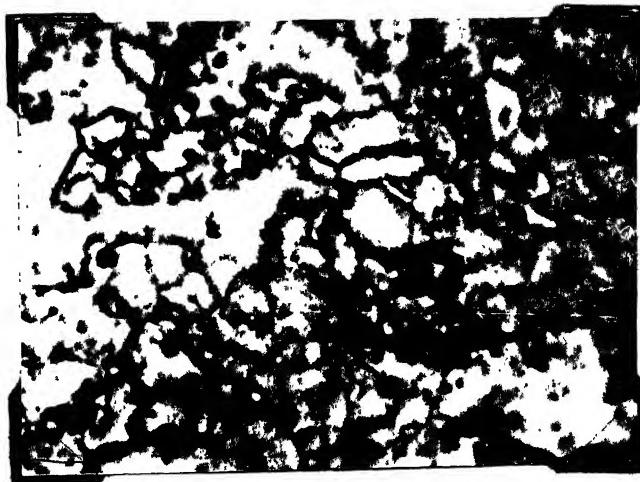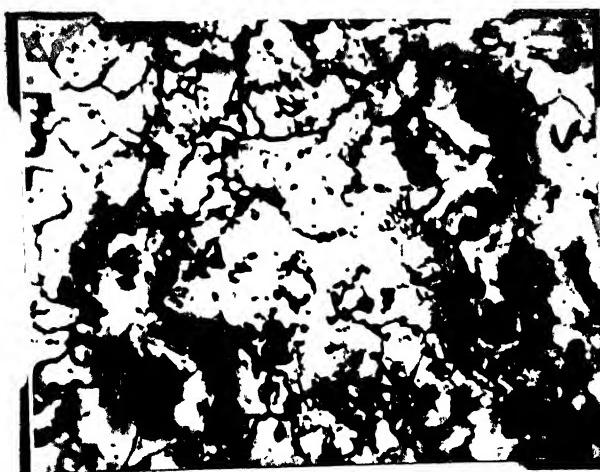(b) Pb-5 V/O Zn

(c) Pb-5 V/O Al$_2$O$_3$

Fig. 3.2   Photomicrographs for composites of Process III
            followed by annealing at 280°C for 2 hrs. (Transverse
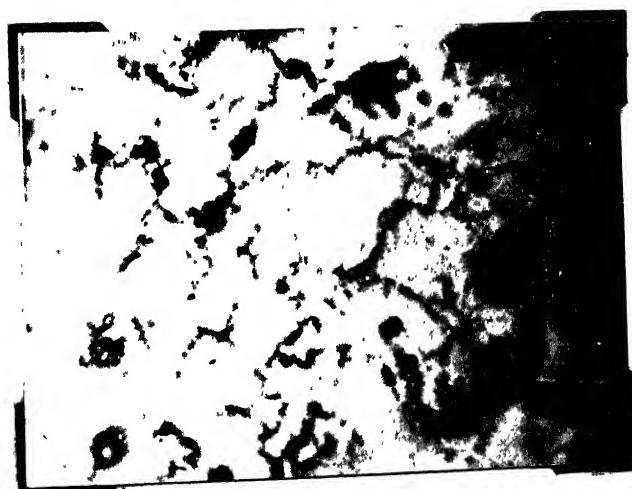   (Magnification -1000X).

(a) P/M Lead

(b) Pb-5 V/O Zn

(c) Pb-5 V/O Al$_2$O$_3$

Fig. 3.3   Photomicrographs for composites of Process IV followed by annealing at 280°C for 100 hrs. (Transverse) (Magnification ~1000X).
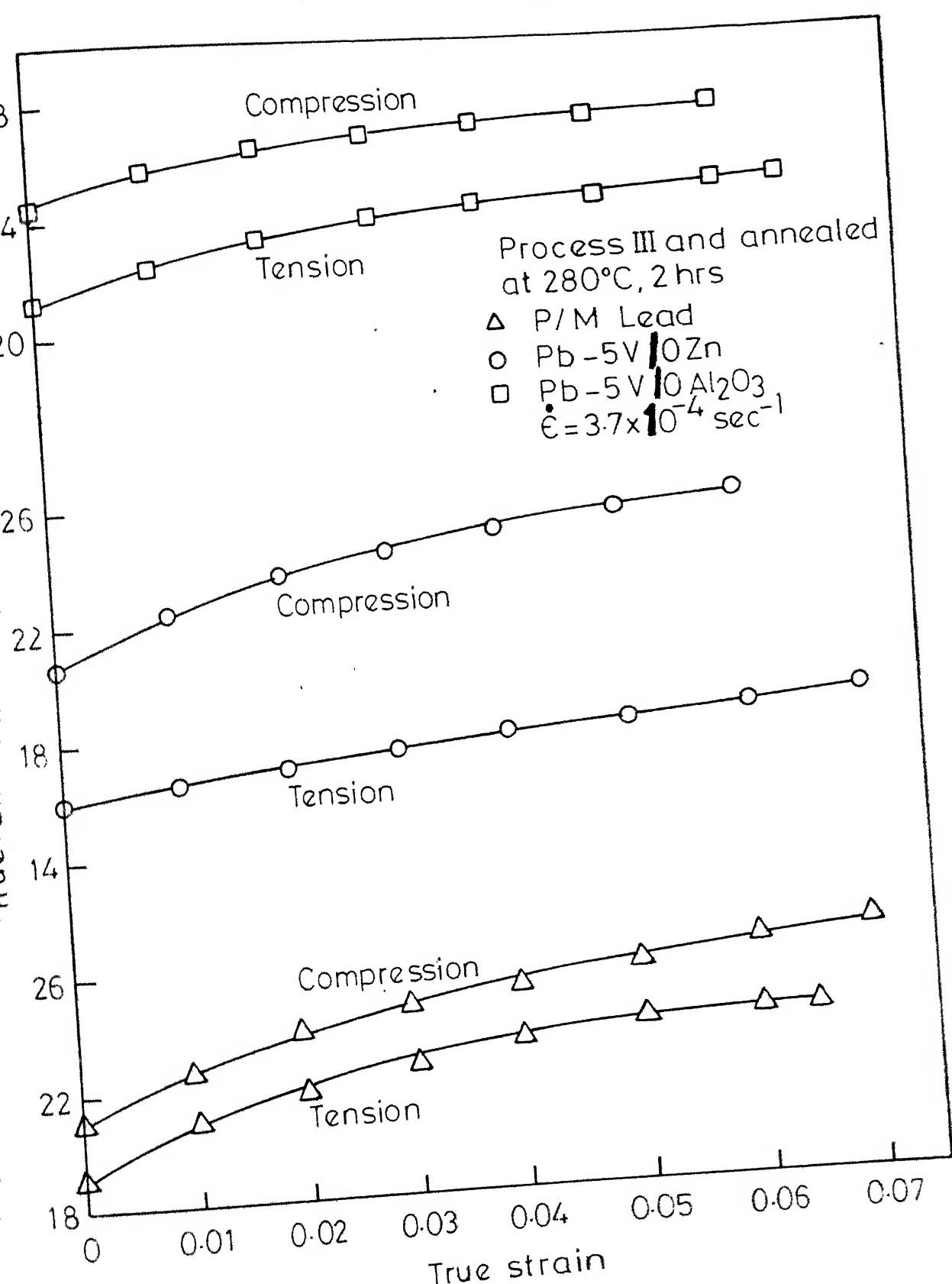
Fig. 3.4 – Typical true stress-true strain curves in tension and compression for Lead-base composites at room temperature.
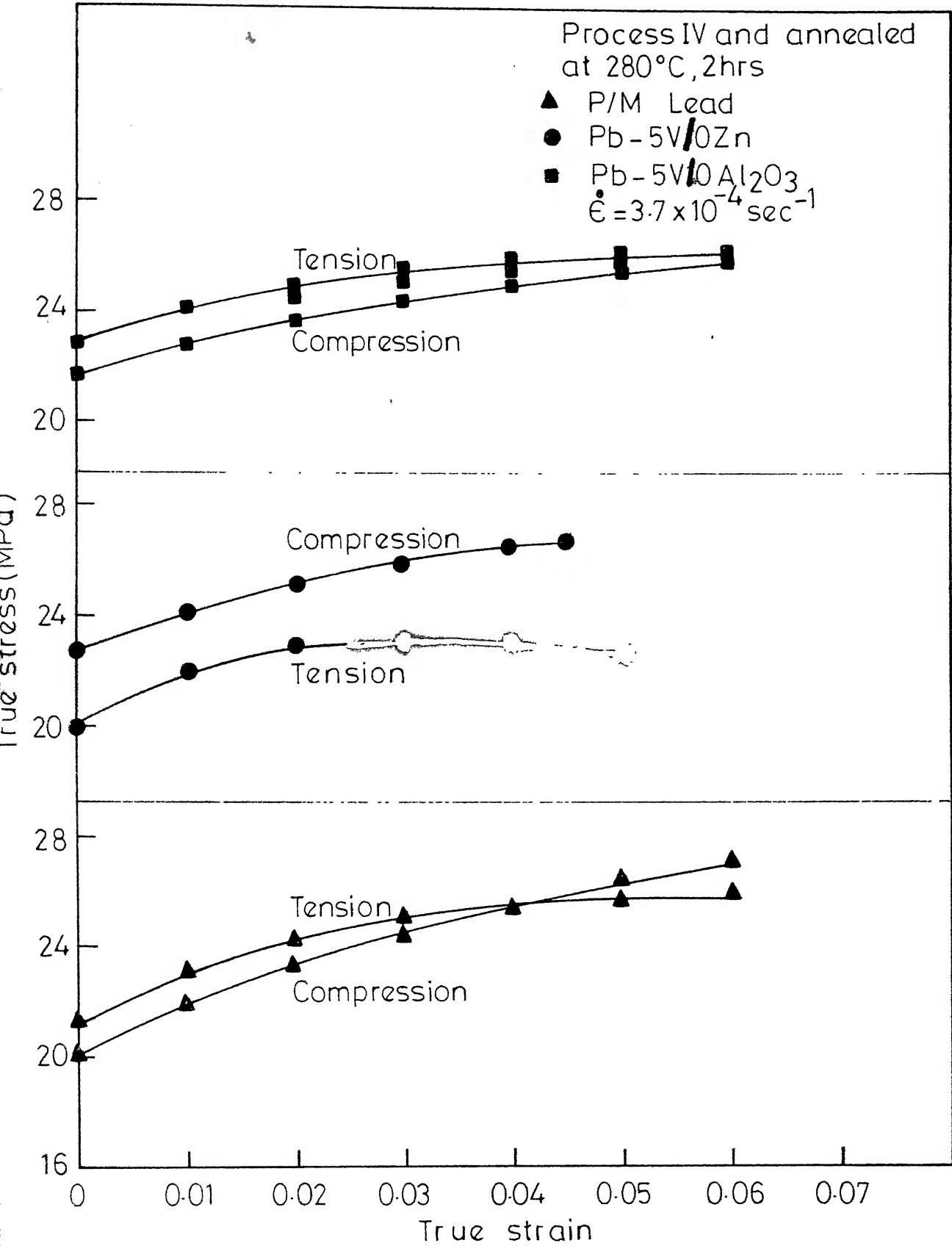
Fig. 3·5 —Typical true stress-true strain curves in tension and compression for Lead-base composites at room temperature.
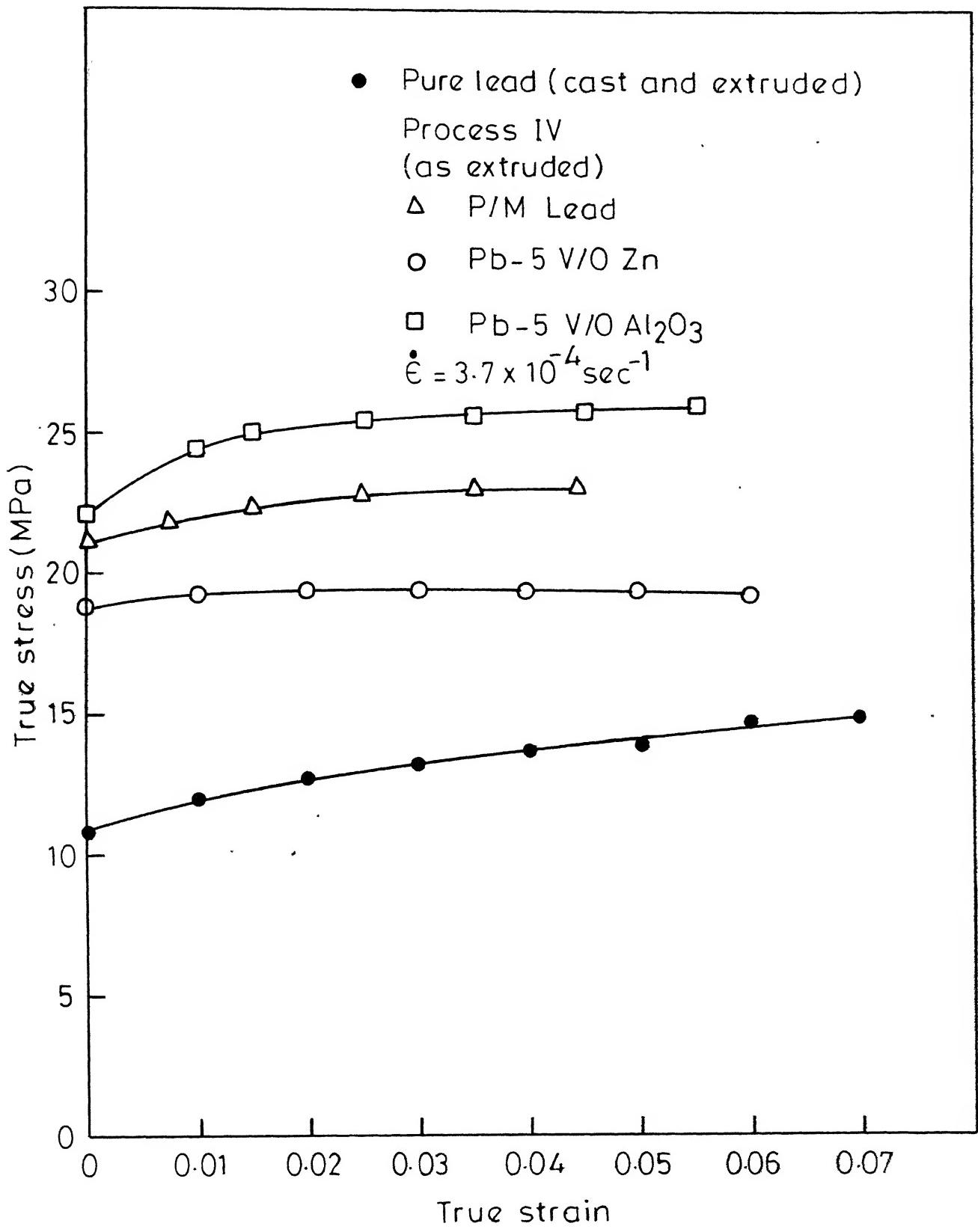
Fig. 3·6 – Typical tensile true stress-true strain curves for
Lead and its composites at room temperature.
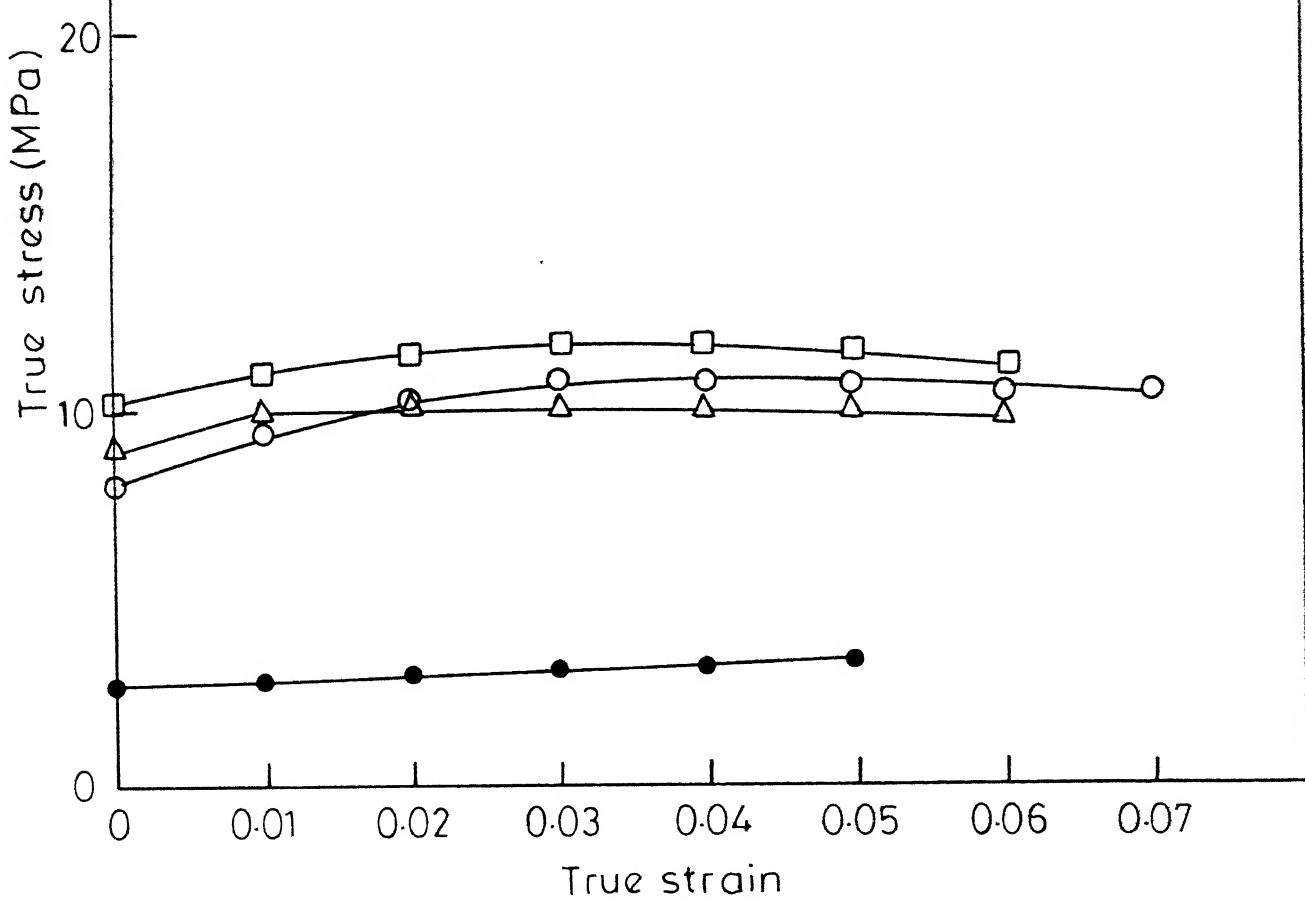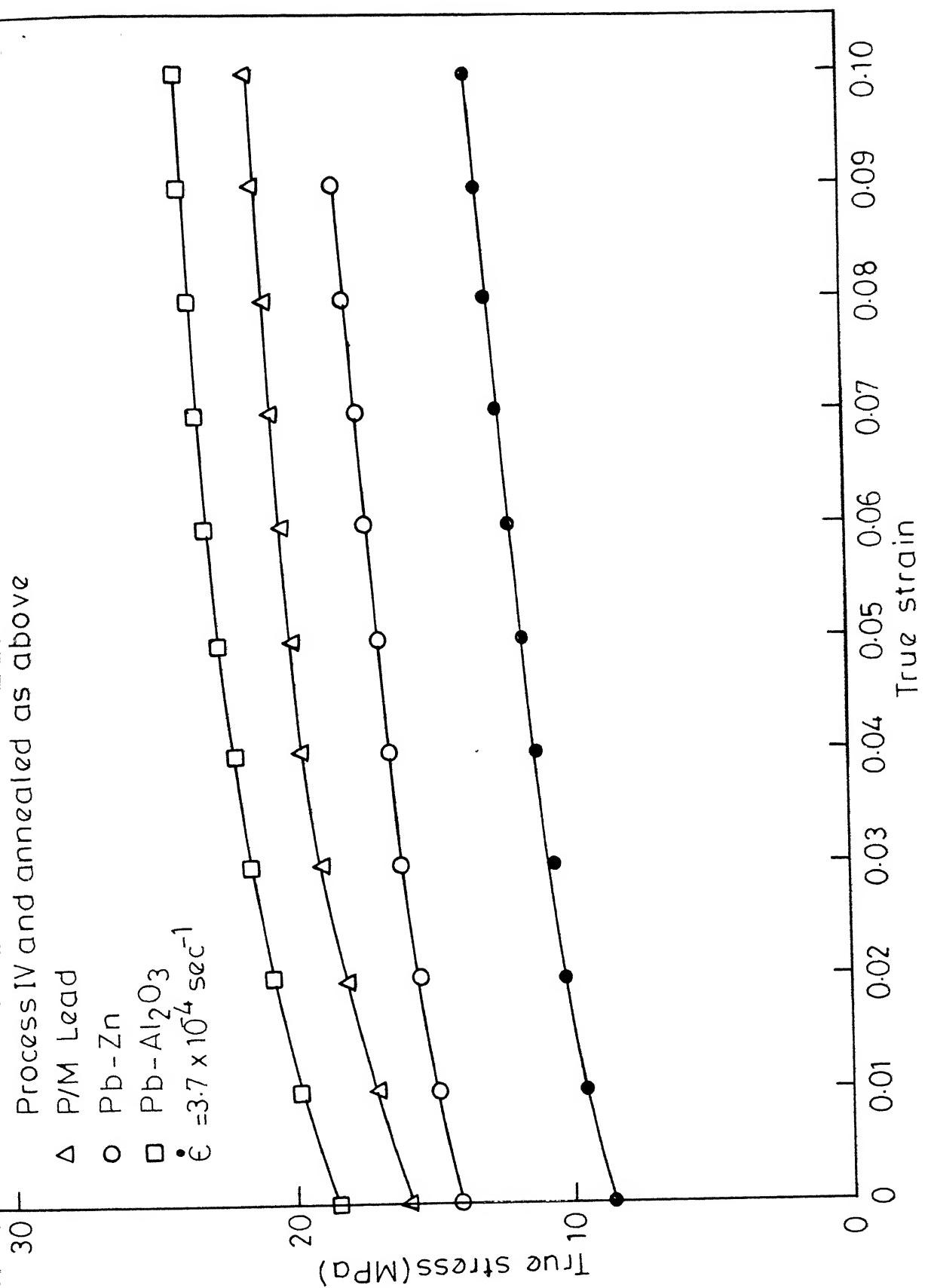
Fig. 3·7 —Typical tensile true stress-true strain curves for Lead and its composites at 180°C.

Fig. 3.8 - Typical tensile true stress-true strain curves for Lead and its composites at room temperature.
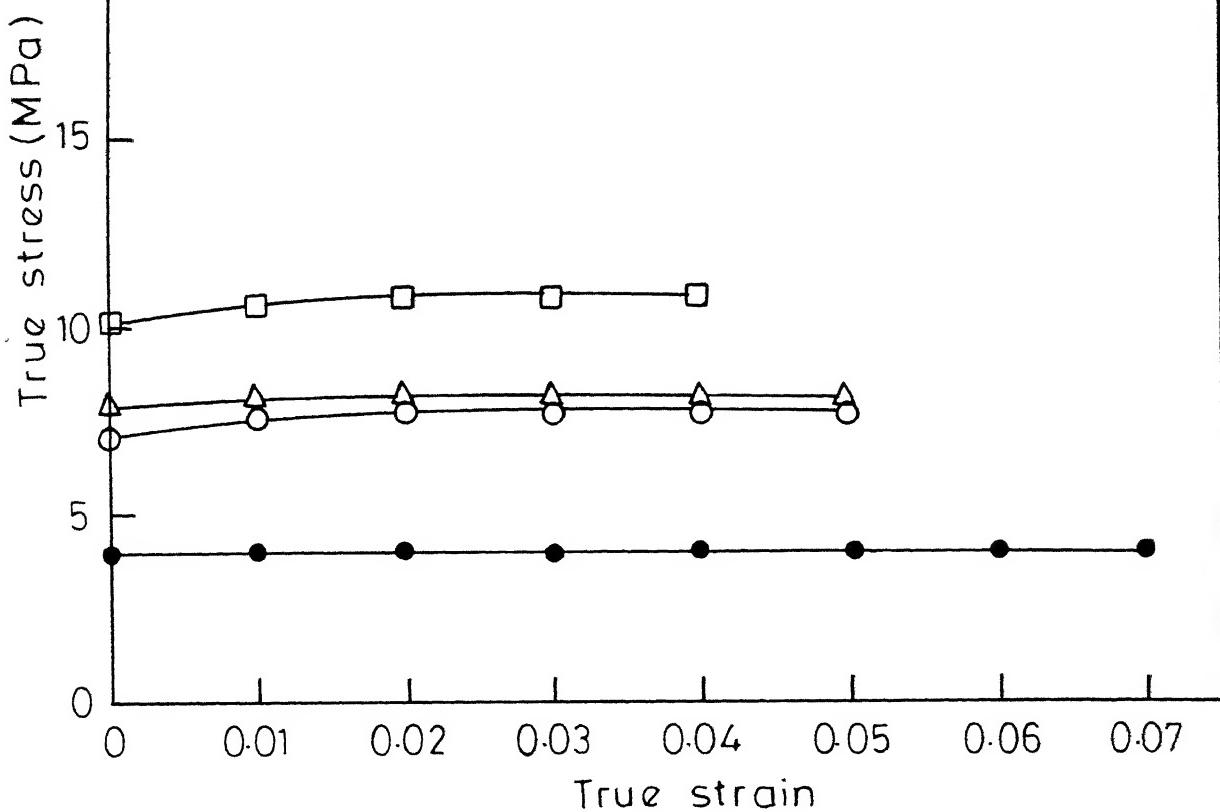
Fig. 3·9 – Typical tensile true stress–true strain curves for Lead and its composites at 180°C.
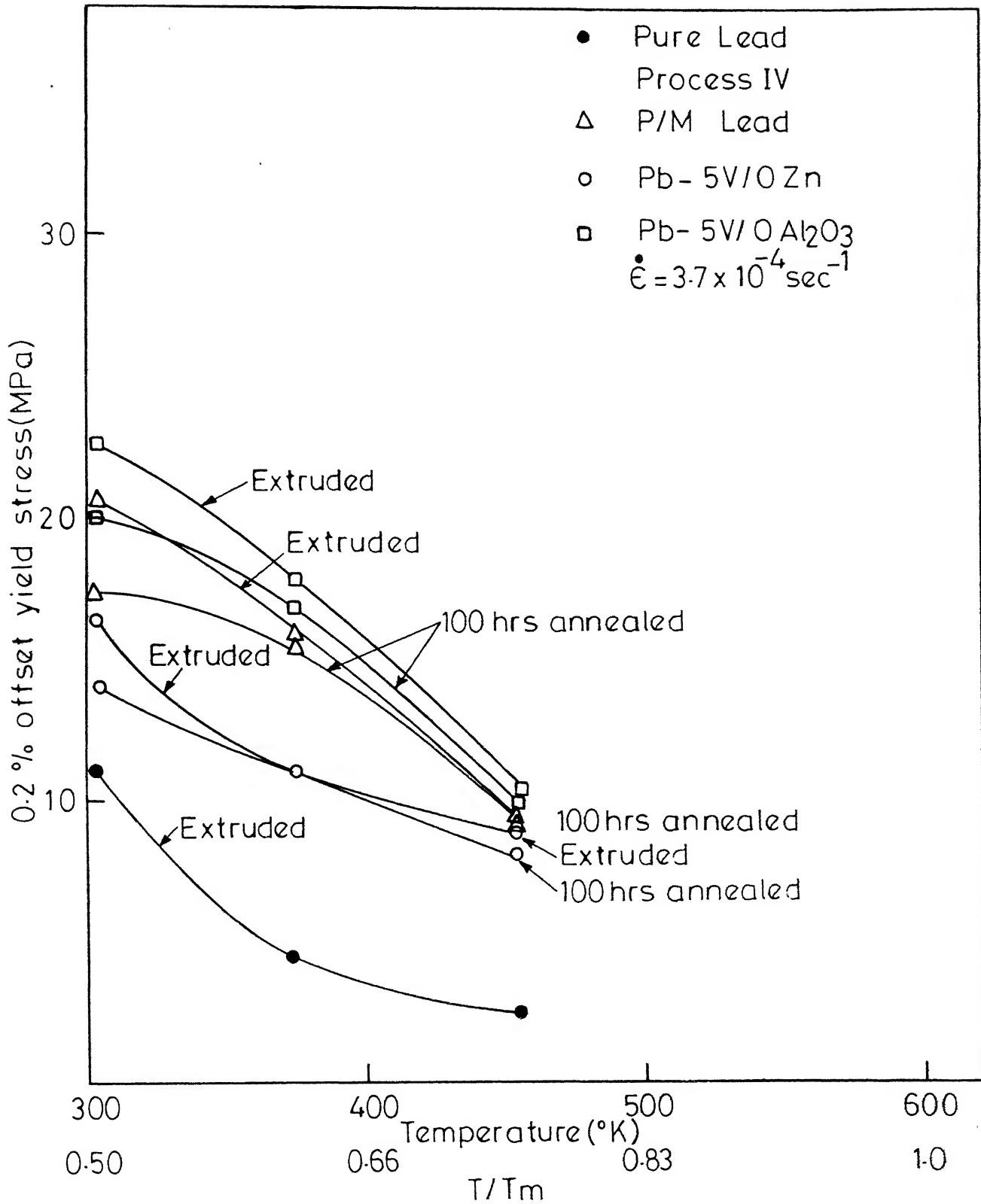
Fig.3·10 –Temperature dependence of yield stress of Lead and its composites in as extruded and 100 hrs annealed condition.
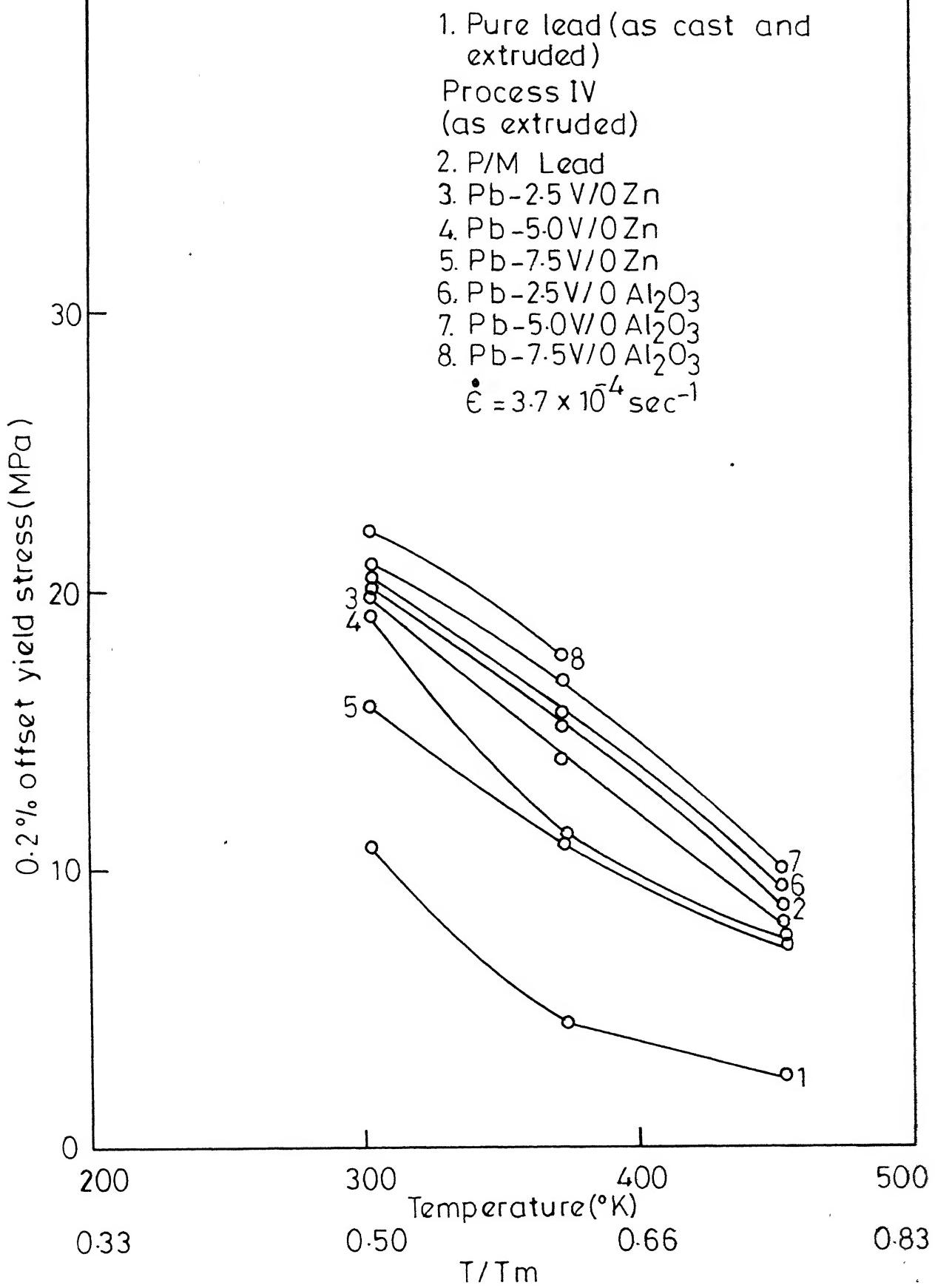
Fig.3.11 – Effect of temperature on 0.2% offset yield stress on Lead and its composites.
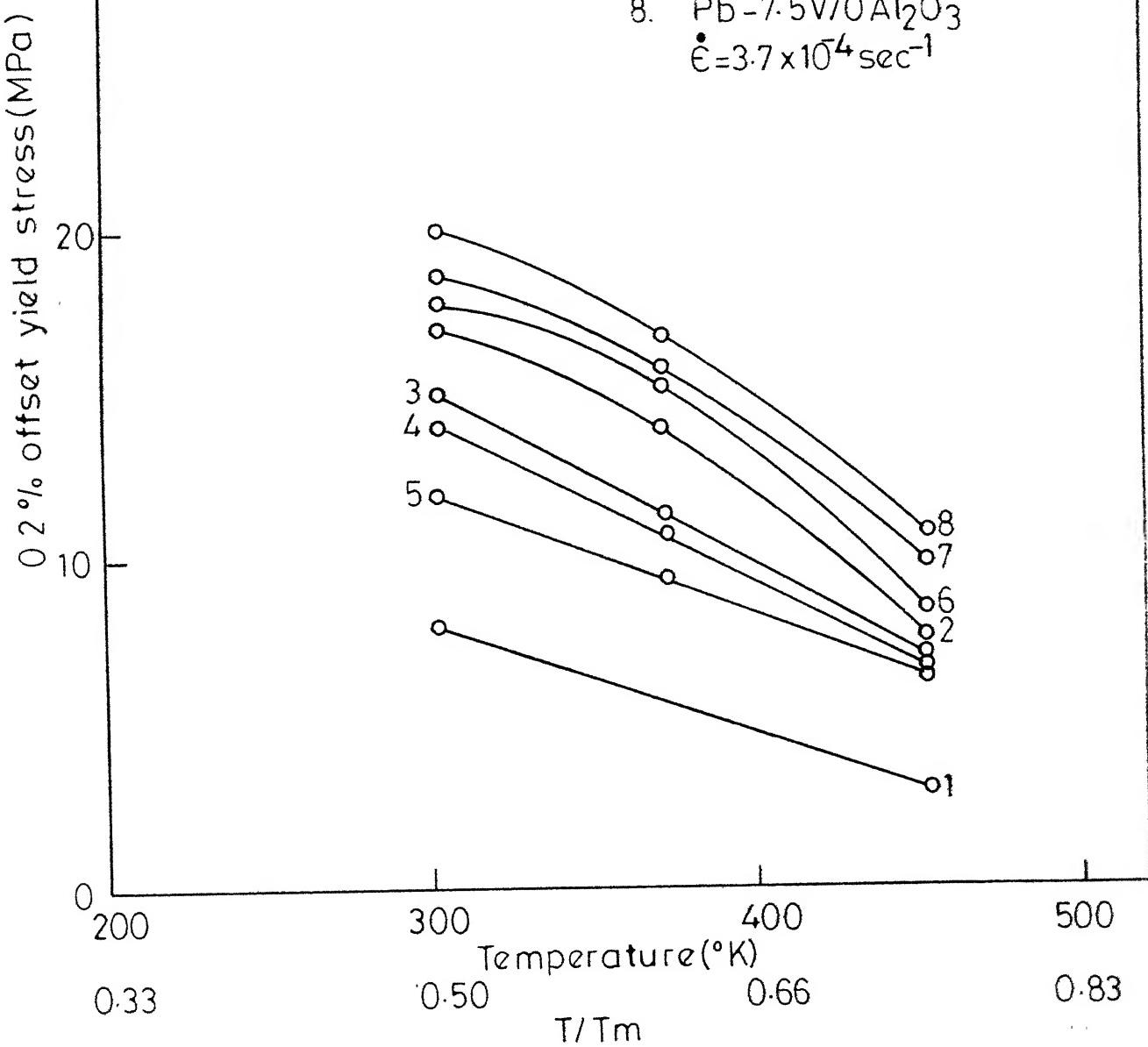
Fig. 3.12 — Effect of temperature on 0.2% offset yield stress of Lead and its composites.
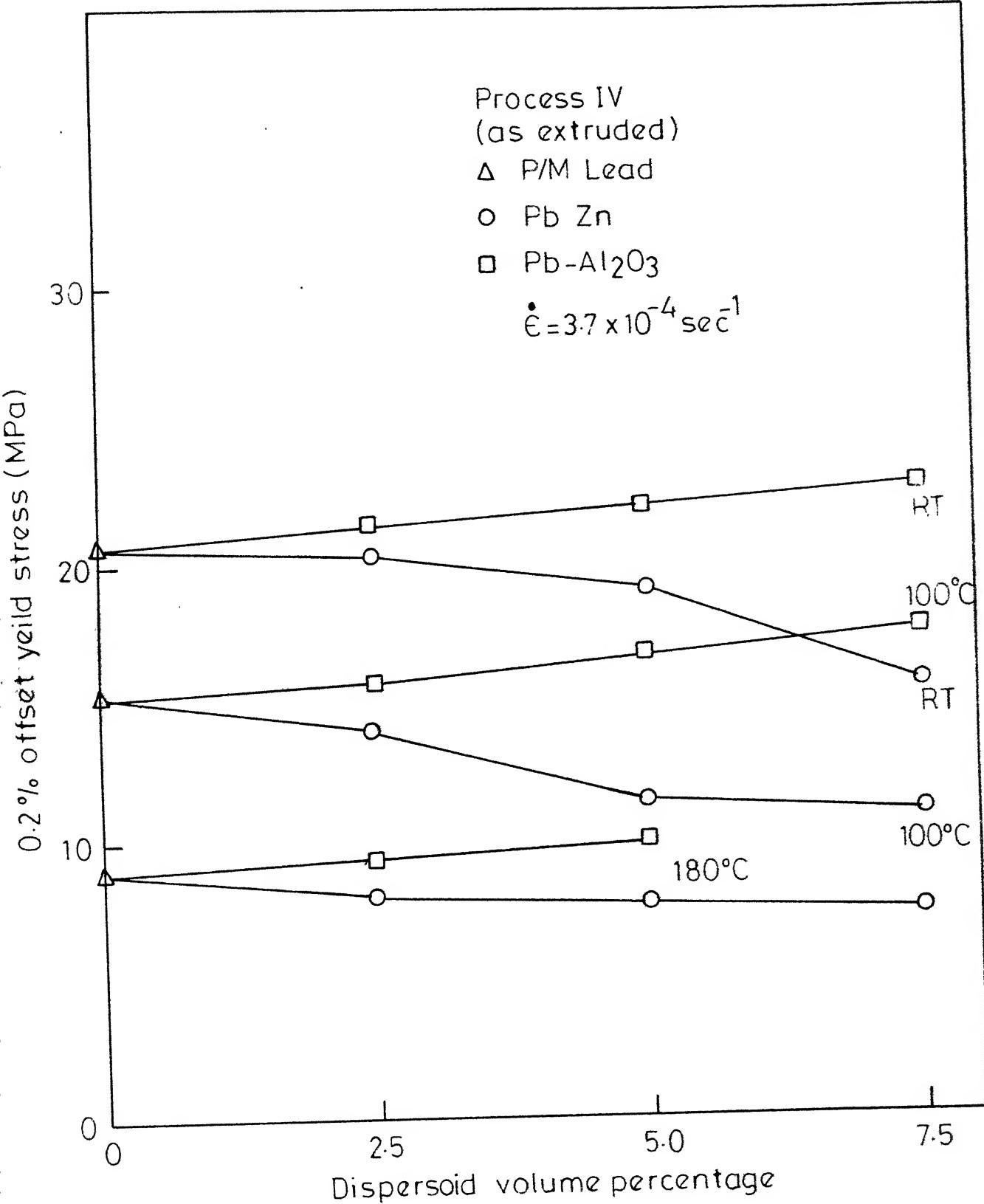
Fig. 3.13- Effect of volume fraction on the 0.2% offset yield stress of Lead base composites at room temperature, 100°C and 180°C.
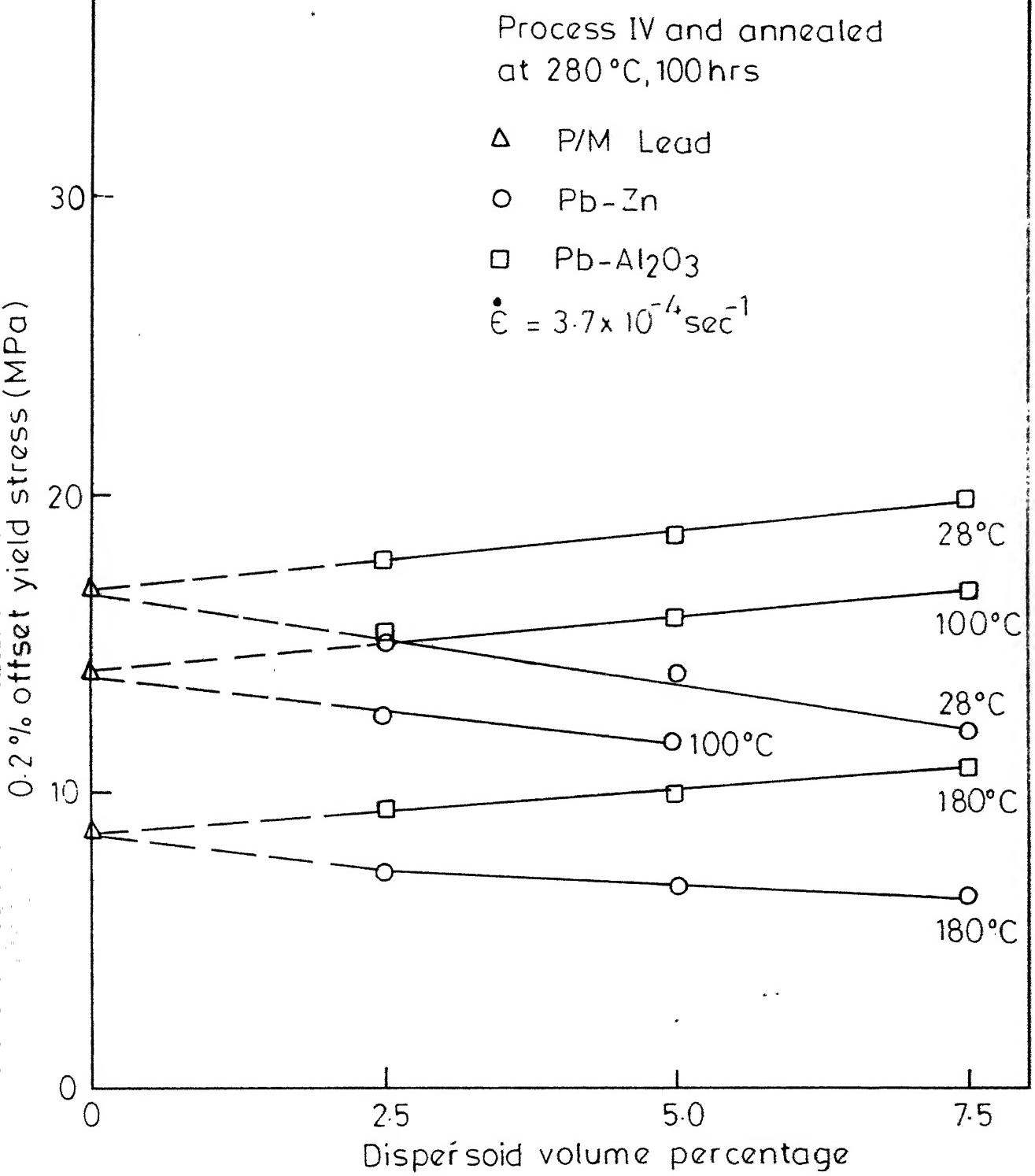
Fig. 3·14- Effect of volume fraction on the 0·2% offset yield stress of Lead-base composites at room temperature, 100°C and 180°C.
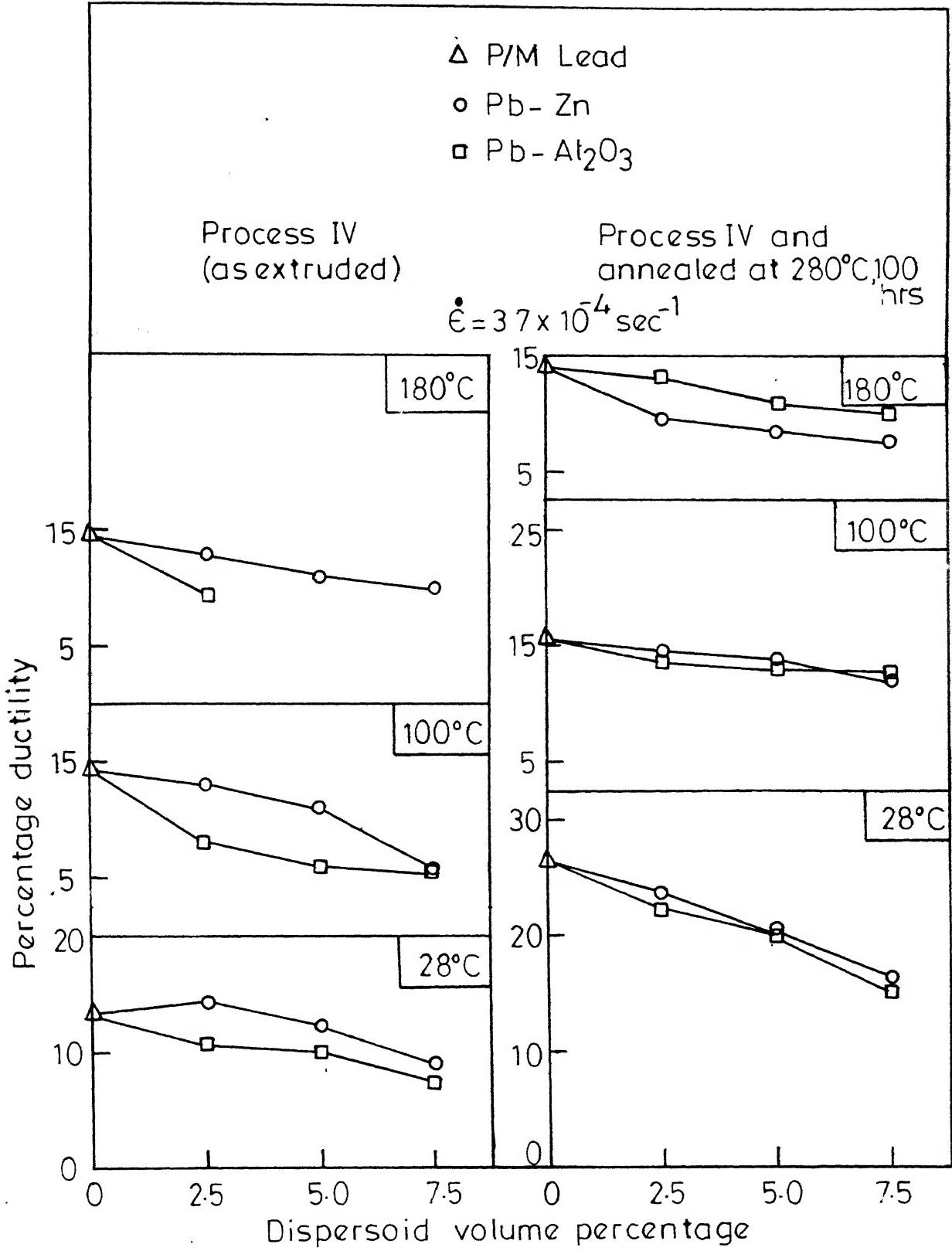
Fig. 3·15 – Effect of dispersoid volume content on ductility of Lead-base composites.
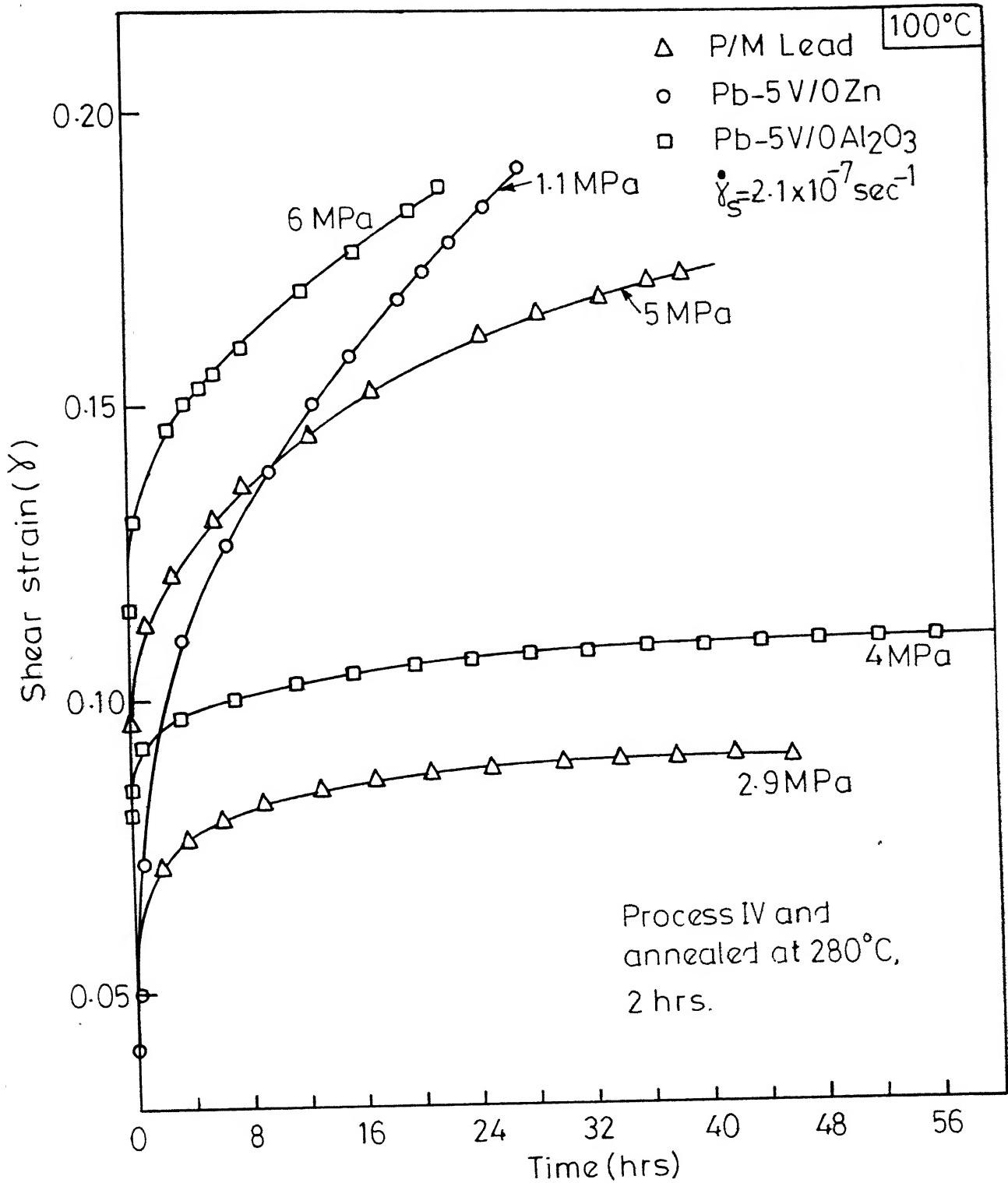
Fig. 3·16 – Typical creep curves for Lead base composites at 100°C for shear stresses below 6MPa.
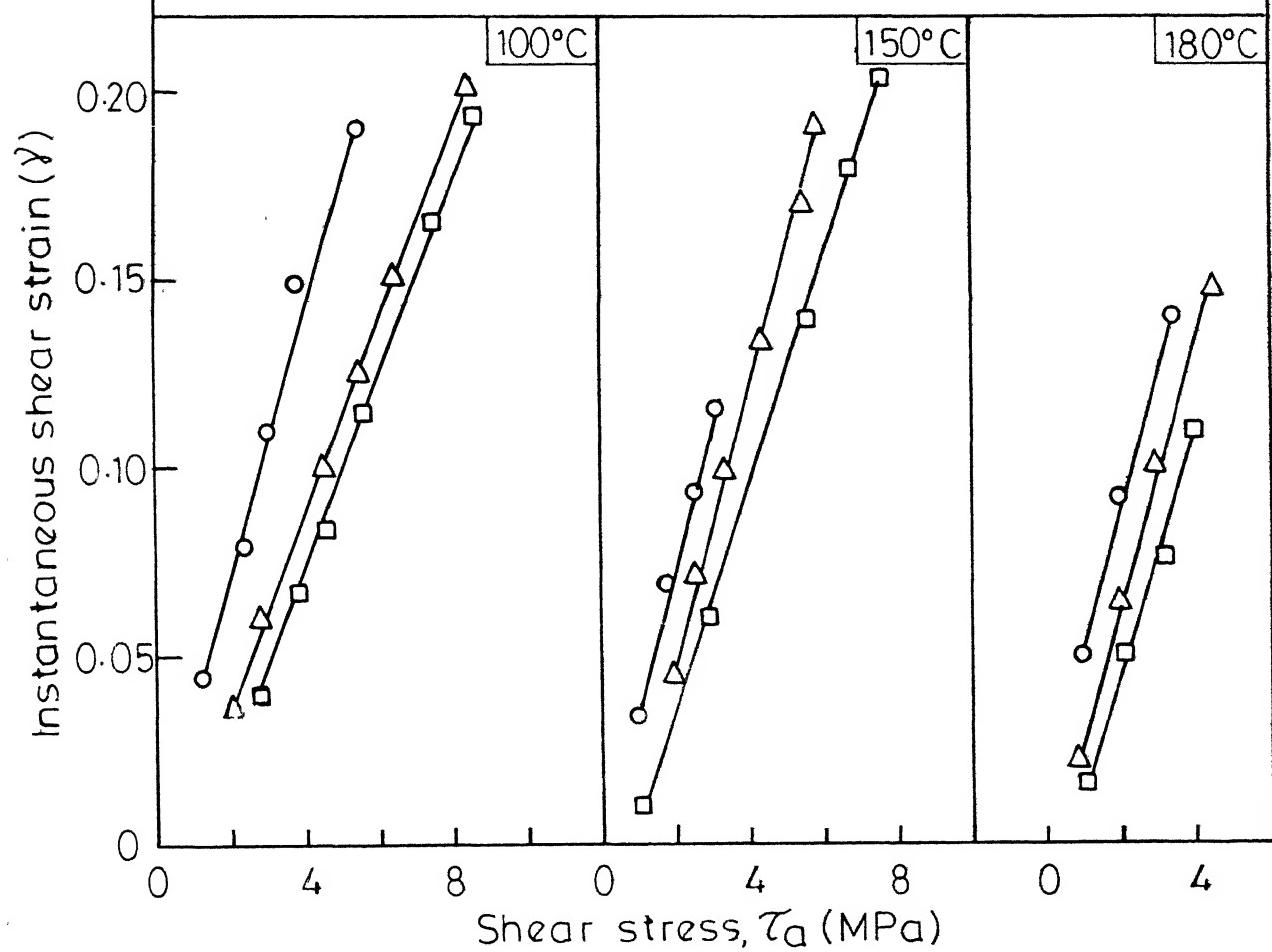
Fig. 3·17 – The shear stress dependence of instantaneous shear strain in Lead-base composites.
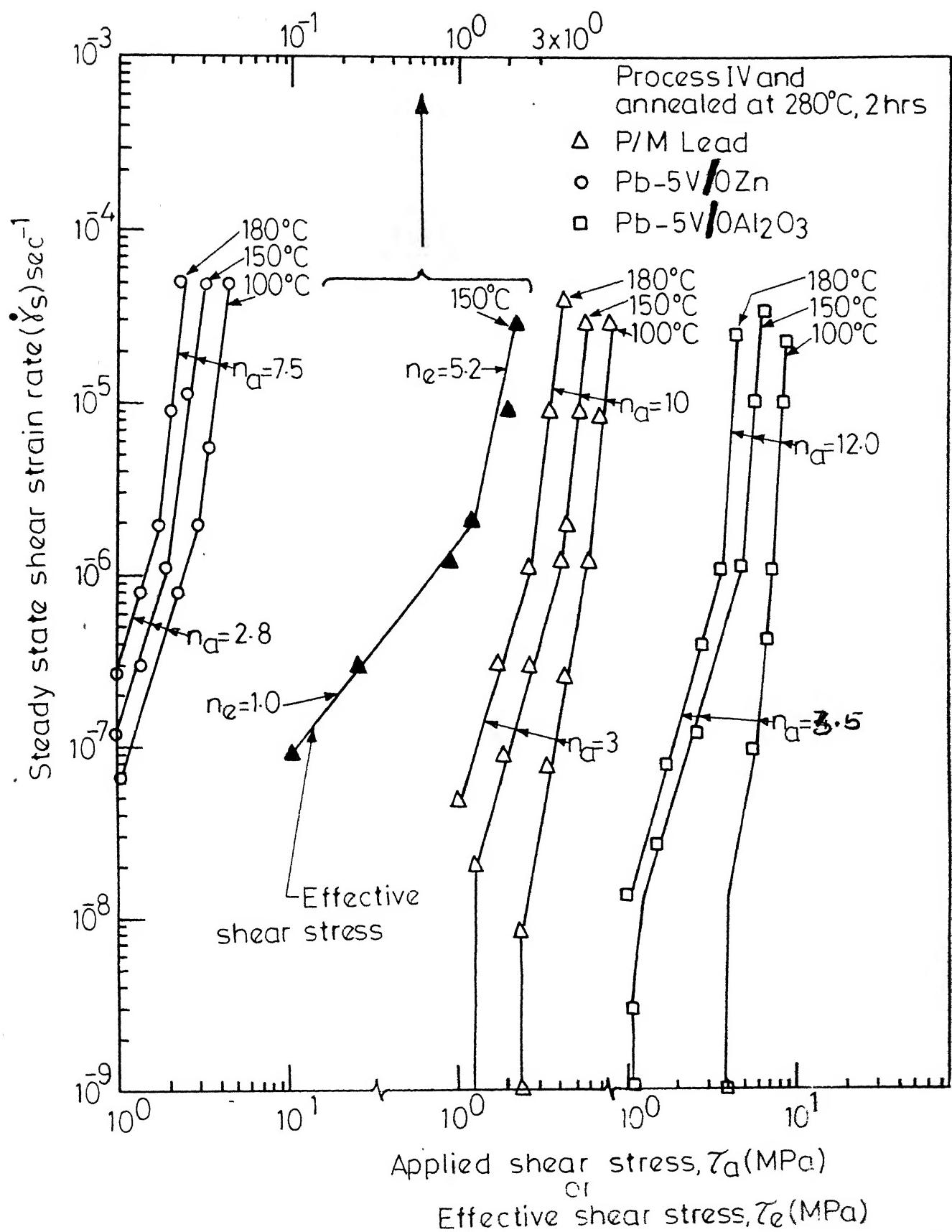
Fig. 3.18 –The stress dependence of the steady state shear strain rate of Lead-base composites.
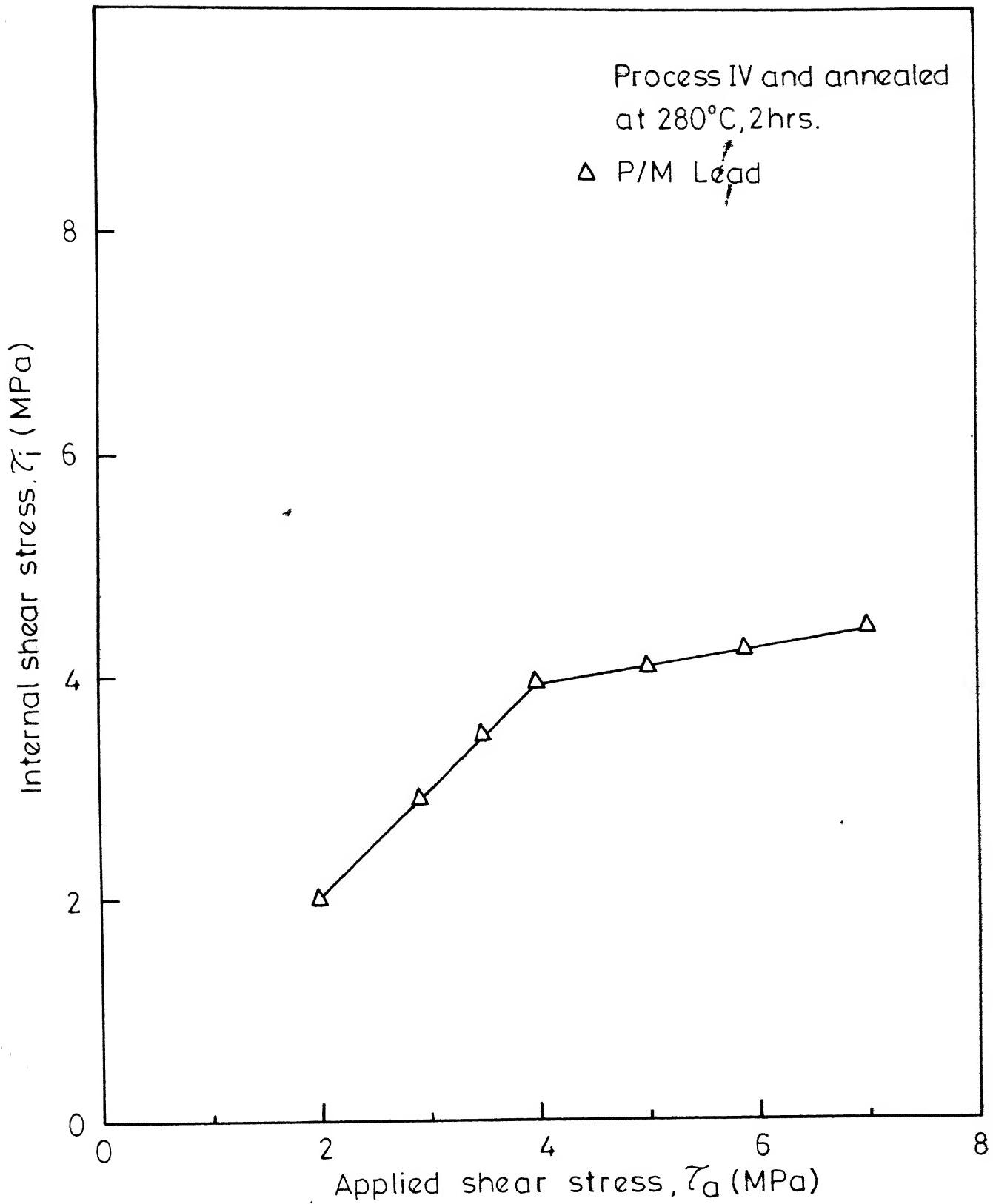
Fig.3·19-Internal shear stress as a function of applied stress
in P/M Lead measured in a creep test at 150°C.
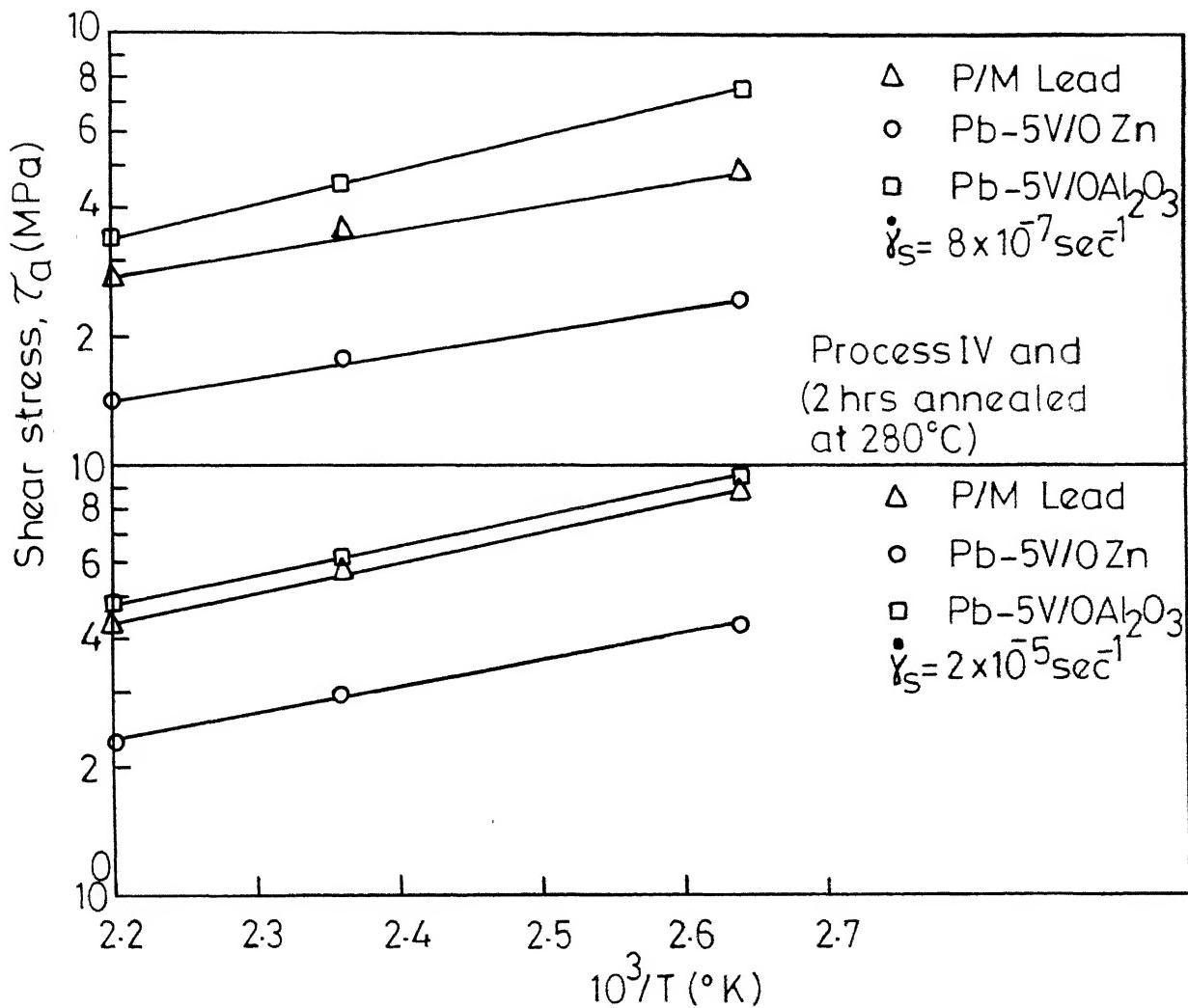
Fig. 3·20 – Activation energies for creep of Lead-base composites as determined by plotting log τ_a vs. 1/T for constant $\dot{\gamma}_s$.

CHAPTER IV

DISCUSSION

The results of the present investigation regarding composite characteristics and mechanical behaviour are discussed in this chapter. The role of powder as well as processing parameters on the characteristics such as porosity, microstructure, compressive strength with its anisotropy are elaborated in Section 4.1. An additional character, namely, SD effect is suggested as the tentative characteristic for determining the structural homogeneity of fully dense P/M products. In Section 4.2, the observed SD effects are discussed in relation to possible mechanisms. The observed normal SD and negative SD effects are explained tentatively on the basis of combined effect of (i) particle-matrix interface bond strength and (ii) residual stresses depending upon the state of the composites. The strengthening as well as weakening observed in the Lead-base composites is explained on the basis of Hall-Petch type relationship. A brief discussion is given about the variation of parameters such as σ_i and k_y in Hall-Petch relation with the temperature and dispersoid nature in Section 4.3. In the last Section 4.4, the threshold stress, low and high stress exponent regions of the creep curve are discussed in terms of GBS mechanism and Ansell-Weertman dislocation climb model.

4.1 Role of Processing Parameters in Characterisation of Lead-base Composites

Full potential of particulate composites prepared through P/M route is realised only when dispersoids in them are properly bonded and uniformly dispersed in the matrix in addition to 'its full density. Production of composites by
attainment of
conventional P/M methods involves usual compaction followed by sintering. The resulting material has a substantial volume fraction of porosity which limits its use in heavy duty as well as structural materials[61]. However, fine grain size is achieved through P/M route in comparison to conventional melting-casting route[62].

Many composites are fabricated by solid state processes under pressure. An important variable in such processes is the amount of plastic deformation imparted through mechanical working[63]. Two different techniques of mechanical working can be considered here, viz. (i) the application of pressure during the powder compaction process and (ii) the deformation processing of consolidated compacts. Increased compaction pressure results in higher densities of green powder compacts. This happens so, because two basic processes occur during compaction of metal powders. These processes are (i) bulk movement of particles and (ii) deformation and fracture of particles. Bulk movement and rearrangement of particles will result in a more efficient packing of the powder. Densification by particle

movement, deformation and fracture implies that the free

space   filled with air is replaced with solid material.

This can take place as long as the air can exit from the

powder mass. Certainly with regard to the production of

high density compacts, deformation is major mechanism of

densification.

As far as bond strength is concerned, depending

upon the nature of the matrix and deformation temperature

(during green compaction as well as deformation processing),

the mechanical and chemical bonds will be developed[64]. In

case of composites, having T_R at room temperature or so,

mass transport through diffusion alongwith the deformation

will be expected, even at room temperature. Further, during

processing of the matrix fibering may take place along the

working direction depending upon the extent of deformation.

The metal matrix in the present investigation, i.e., Lead

is having T_R (0.51 T_m) at room temperature. Hence, both the

bonds, namely, mechanical and chemical are expected in

composites prepared through Process I. However, contribution

from chemical bond presently will be lesser in comparison

to mechanical bond arising through interlocking and

frictional effects. Moreover, in Process II, additional

deformation through swaging is given which modifies the

bonding as well as introduces further fibering. Hence, the

observed increment in densification, compressive strength

and fibering of matrix after Process II over Process I are in agreement with the argument forwarded above.

Now, in case of compacted and sintered products, the additional elimination of porosity is achieved through thermal processing. Here, thermal processing constitutes of sintering as well as further annealing after extrusion. During sintering, densification takes place apart from the change in shape and size of the pores. Rounding of the pores with reduction in their number is observed[65]. On this basis, the observed porosity level of composites after Process III over that of Process II can be rationalised.

Further, the reflection of the improved bond strength is observed through improvement in the extrusion pressure of Process III composites over those of composites prepared through Processes I or II (Table 3.6). Moreover, density and compressive strength variation is reduced further which is an indication of increased homogeneity (Table 3.5 and 3.8) Thus, it can be inferred that uniform density, higher extrusion pressure and compressive strength of Process III composites in comparison to the composites of Process II are the consequences of the additional sintering stage introduced in Process III.

Generally, deformation processing of particulate composites ends in fibering of the metal-matrix and the dispersoids will be aligned (or stringered) in the direction

of deformation depending upon the processing history[66,67].
Here, processing parameters of utmost importance are
compaction pressure, nature of the dispersoid, powder
preparation route[68] and thermal processing of the deformed
(extruded) composites. The compaction pressure is important
at the initial stage of the processing. Depending upon the
extent of compaction pressure and nature of the particle,
the microstructural distribution will be influenced. At low
compaction pressure, the dispersoids will be mostly at the
surface or just inside the metal powder particles. However,
at high compaction pressure, the probability of penetrating
the matrix grains by dispersoids would be more for hard
particles than soft ones. From the reported literature[68-70],
the importance of powder preparation route, indicative of
interfacial bond strength between matrix and dispersoid, may
be judged. In case of composites prepared through internally
oxidised powders, the interfacial bond strength is better
in comparison to the composites prepared through mechani-
cally mixed powders[68]. As a consequence, less extent of
dispersoid dragging towards the matrix grain boundaries is
observed in the composites prepared through internally
oxidised powders in comparison to those prepared out of
the mechanically mixed powders[68]. Further, the hardness
of the dispersoid will also alter the microstructural
features[68-70], such that hard particles would be

dragged to a lesser extent towards grain boundaries in comparison to soft ones during thermal treatment. In total, if the dispersoids are dragged towards the grain boundaries, its ability in restricting the grain growth will be adversely affected. The outcome of it is the expected grain growth in the composites which is reflected presently in our study on Pb-5 V/O Zn composites (Figures 3.2 and 3.3). The observed dispersoid distribution (Figures 3.2 and 3.3), extrusion pressure (Table 3.6), compressive strength (Table 3.8) and its anisotropy (Table 3.9) of the composites prepared by Processes III and IV are thus, the outcome of the processing history, particle nature as well as powder preparation route as discussed above.

A noteworthy feature of the present investigation is that SD effect has been exhibited by all the composites prepared through Processes III and IV (Figures 3.4 and 3.5). Despite the low porosity level of the investigated Lead-base composites, there has been significant SD in them. This indicates the importance of factors such as particle-matrix interface bond strength[28] and residual stresses[71] apart from the porosity[72] in causing SD. Moreover, there has been considerable reduction in SD for composites prepared by Process IV in comparison to those by Process III. Improved bond strength due to higher compaction pressure adopted in Process IV appears to be the main cause of this reduction in SD.

4.2 Strength Differential (SD) Effect

It is apparent that the Lead-base particulate composites have exhibited a strong strength differential effect. Hence, the SD effect is not unique to TD-Nickel among particulate composites prepared by the P/M route[28]. The strength differential effect in these Lead base composites varies from process to process as well as from one composite to the other.

The P/M products are generally associated with the porosity which reduces the load bearing capacity of the composites in tension. In such cases, tensile yield strength values are adversely affected in comparison to compression. This results in the strength differential effect, the magnitude of which depends on the level of porosity. The porosity contribution to the SD effect may be estimated as follows:

The strength of a porous P/M material with a very ductile matrix capable of relaxing stress concentration is given by[x]

$$\sigma = \sigma_0 \ (1 - KP^{2/3}) \tag{4.1}$$

---

x T.J. Griffiths, R. Davies and V.B. Bassett, Powder Met. Vol. 22 (3), 109 (1979).

where σ = tensile strength of porous material

σ_0 = tensile strength of pore free material

K = constant depending upon the pore morphology and matrix material

and P = Porosity fraction

The values of K range from 0.98 to 1.3[X]. For soft materials having least anisotropy, K is assumed to be unity. Hence the equation (4.1) can be rewritten as

$$\sigma = \sigma_0 \ (1 - P^{2/3}) \qquad (4.2)$$

It is further observed that in pore free materials yield in compression (σ^C) is generally equal to yield in tension (σ^T). Hence the equation (4.2) can be written as

$$\sigma^T = \sigma^C \ (1 - P^{2/3}) \qquad (4.3)$$

Hence,

$$\% \ SD = \frac{\sigma^C_{0.2\%} - \sigma^T_{0.2\%}}{\sigma_{0.2\%}} \times 100 = P^{2/3} \times 100 \qquad (4.4)$$

In the present Lead base composites, the estimated SD effect values for all the composites due to porosity are given in Table 3.10. It is clear from the Table 3.10 that the

---

x T.J. Griffiths, R. Davies and V.B. Bassett, Powder Met. Vol. 22 (3), 109 (1979).

contribution towards SD due to porosity is small. Hence, porosity cannot account for the observed SD. Having deducted the contributions due to porosity, the net SD effects are summarised in Table 3.10. The table contains, the observed SD effect, SD effect due to porosity and net SD effect for Processes III and IV.

Several possible mechanisms[28,73-77] for explaining the observed net SD effect in various materials have been suggested. These are: particle-matrix interface rupture[28], residual stresses[71], transformation of retained phases[73], opening of microcracks[74], internal Bauschinger effect[75], non-linear solute dislocation interactions[76], diffusion coefficient variation with hydrostatic pressure[77] and twinning[77]. Among these possible explanations offered for SD effect, some of the explanations are not relevant here for the following reasons. These Lead base particulate composites are devoid of retained phases[73], solute-dislocation interaction[76] and twinning[77]. Moreover, the matrix metal being ductile, opening of microcracks[74] during deformation of Lead base composites is not likely to be an important mechanism. As far as SD effect due to the effect of hydrostatic pressure on the diffusion coefficient[77] is concerned, the extent of the SD effect is estimated to be less than 2 %, for composites under study. Hence, the

above mechanism offered for explaining the SD effect in other materials would not explain the observed SD in the present study.

The net SD effect can, now be examined in light of the remaining mechanisms, viz., (i) particle-matrix interface rupture[28], (ii) residual stresses[71] and (iii) internal Bauschinger effect[75].

Olsen and Ansell[28] have shown that the tensile yield strength of some two phase alloys is directly related to the strength of the interfacial bond between the two phases. They found that in TD-Nickel this could result in a tensile yield strength lower than the compressive yield strength, and attributed this SD effect to the separation of the particle-matrix interface in tension at a stress below the normal yield stress. The observed normal SD effect in Lead-base composites prepared through Process III could be explained on the basis of particle matrix interface separation.

It follows from the particle-matrix interface rupture model that the SD would decrease by improving the bond strength. The improvement in bond strength can be achieved either by improving mechanical bonding or chemical bonding (solid solution alloying)[28]. In the present

investigation through greater compaction pressure, the
mechanical bonding has been improved in composites
prepared   by   Process IV. The improvement in bond
strength, perhaps has resulted in the reduction of the SD
effect in the composites prepared by· Process IV. However,
in the case of P/M Lead (containing PbO) and Pb-Al$_2$O$_3$
composites prepared ˙ by _ Process IV, the observed
negative SD effect cannot be explained on the basis of
this mechanism only.

In the case of particulate composites, the primary
origin of residual stresses[71] is two fold: thermal and
mechanical. The former arises from the differing thermal
coefficients of expansion of the matrix and dispersoids.
During cooling of such composites, thermal stresses are
developed. The extent and sign of these stresses depend upon
the nature of the dispersoid with respect to matrix[15,79].
Thermal stresses may be compressive or tensile in nature.
When $\alpha_m \cdot > \alpha_p$, where α_m is matrix thermal coefficient of
expansion and α_p particle or dispersoid thermal coefficient
of expansion, a radial compressive stress field is developed
around the dispersoid[79] on cooling to room temperature from
a higher temperature. When such a material is tested in
tension, it will require higher tensile stress to start the
deformation or yielding and reverse will happen while

testing the same material in compression. In other words, a negative SD effect would be exhibited when $\alpha_m > \alpha_p$. On the contrary, when $\alpha_m < \alpha_p$, the materials will have higher yield values in compression than in tension. In such cases, the normal SD effect is expected.

In the present case, Zinc, Alumina and PbO with particle sizes of 1.2 μm, 1 μm and 0.5 μm (see Figure 3.3 for size of PbO particle) respectively are present. These sizes are quite large and provide sufficient ground to invoke the presence of thermal stresses provided their thermal coefficients differ widely from that of the Lead matrix material. In the case of Zinc dispersoids, $\alpha_{Zn} \simeq 1.04 \, \alpha_{Pb}^{80}$ and the estimated[xx] thermal residual stress is 0.25 MPa and it would be tensile in nature. The tensile residual stress in the case of Pb-Zn would lead to normal SD effect. However, the residual stress being small, its contribution to the normal SD would be expected to be small. On the basis of these thermal stresses it would not be possible to explain the observed SD effect in the Pb-Zn composites prepared by both the Processes III and IV.

In the case of Al_2O_3 dispersoids, $\alpha_{Pb} \simeq 3\alpha Al_2O_3^{80}$ and for PbO, $\alpha_{Pb} \simeq 1.8 \, \alpha_{PbO}$. The estimated[xx] thermal residual

---

xx   Gelbert W. Brassell and Kenneth B. Wischmann, J. Mat. Sci. Vol. 9, 307 (1974).

stresses for Pb-Al_2O_3 and P/M Lead (containing PbO) are
7.3 and 4.8 MPa respectively. The nature of these stresses
would be compressive and would lead to negative SD effect.
These thermal stresses would thus qualitatively explain the
observed negative SD effect in the composites containing
Al_2O_3 and PbO prepared by Process IV.

However, the normal SD effect in composites
containing Al_2O_3 and PbO prepared by Process III cannot be
explained if such thermal stresses alone are controlling
the yield behaviour.

The second source of residual stresses in the
materials is of mechanical origin. As far as mechanical
residual stresses are concerned, these arise during
deformation processing of a material. There is usually
some degree of inhomogeneous deformation during processing
which leads to residual stresses. Materials containing
mechanical residual stresses are expected to exhibit
Bauschinger effect[75]. Yield strength of the material would
be lowered in the direction opposite to the direction of
prior strain (during processing). For example, compressive
yield strength of an extruded material would be lower than
tensile yield strength if the axis of testing is parallel
to the extrusion direction. It would thus result in a

extent of SD is seen in Zn containing composites prepared by Process IV. In Al_2O_3 and PbO containing composites, the thermal stresses give rise to a negative SD effect. Hence, the contribution from mechanism (i) will oppose that due to (ii). In these composites prepared by Process III, normal SD is observed even though both the mechanisms (i) and (ii) are in operation. The reason behind it is the dominance of mechanism (i) over (ii). On the other hand, in the composites prepared through Process IV, there is an improvement in bond strength, mostly due to the high compaction pressure applied during processing. This improved bond strength will lead to the elimination of SD in these composites, if only the particle-matrix interface rupture mechanism were responsible for SD. But negative SD effect is observed in these composites (Table 3.10), which may be due to dominance of the thermal stress effect (mechanism (ii)).

For the Process IV composites in the as extruded state, the net SD shown in Table 3.10 can be explained on the basis of mechanisms (i), (ii) and (iii). Since the contribution from mechanism (ii) is negligible in Zn containing composites, the main sources for the observed SD are mechanisms (i) and (iii) only. Here, contribution from mechanism (i) will oppose that due to (iii) and thus we see reduction in the extent of net SD effect over that of composites annealed for 2 hours as shown in Table 3.10. The normal SD effect observed in the as extruded Zn

containing composites is a clear indication of the dominating role of mechanism (i). On the other hand, all the three above mentioned mechanisms are expected to play an important role towards SD in Al_2O_3 and PbO containing composites of Process IV in the as extruded state. Here again, contribution from mechanism (i) will oppose that due to mechanisms (ii) and (iii) and thus, we see an increased negative SD effect over the composites annealed for 2 hours.

Further, all the three factors responsible for SD are expected to depend on the nature and volume fraction of the dispersoids. Consequently, the extent of the contributions from these three mechanisms towards SD will be altered with the volume fraction of the dispersoids as well as the processing history (as extruded and 2 hours annealed at 280°C). Thus, the overall observed SD effects in these composites can be rationalised on the basis of the interplay of particle-matrix interface rupture mechanism[28], thermal[15,79] and mechanical residual stresses[71] (internal Bauschinger effect[75]).

As far as variation of SD with strain is concerned, the extent of SD increases with strain in all the Process III composites (Figure 3.4). This observation is in agreement with the proposal that in Process III composites, matrix-particle interface rupture mechanism dominates the deformation behaviour. The same is true for Zn containing composites of Process IV (Figure 3.5). However, in PbO and

Al_2O_3 containing composites of Process IV, there is a competition between both matrix-particle interface rupture and thermal stress mechanisms during straining. Here, the latter mechanism opposes the effect of the first. During tensile deformation, the extent of SD increases with the strain due to matrix-particle interface separation mechanism. On the other hand, the residual stress (thermal or mechanical) effect causing negative SD is likely to be less important at larger strains due to possible modifications of these residual stresses through plastic deformation leading to a reduction in the magnitude of SD with strain. The experimentally observed trend of cross-over of compressive and tensile stress-strain curves in the P/M Lead and $Pb-Al_2O_3$ composites prepared by Process IV are possibly the manifestations of the above effects (Figure 3.5). Further clarification is also likely to be important in altering the SD with strain.

4.3 Yield Behaviour of Lead-base Composites

As far as yield behaviour is concerned, all the composites including P/M Lead have exhibited higher 0.2% offset yield strength over pure Lead prepared through conventional (casting and mechanical working) route. However, in comparison with P/M Lead, Pb-Zn composites have shown lower yield strength and $Pb-Al_2O_3$ marginally higher strength.

Strengthening in metal-matrix particulate composites has been explained in terms of such micro-mechanisms as (i) direct strengthening[21-23], where direct particle dislocation interactions account for strengthening, (ii) indirect strengthening where particle stabilises small grain size and/or dislocation substructure[25] or such macro-mechanisms as (i) constrained plastic flow[13], (ii) load sharing by dispersoids[13]. As far as the macro-mechanisms are concerned, these are not applicable to the present case since volume fractions of dispersoids used in present composites are quite low (< 0.10) and would be unable to effectively constrain plastic flow or share external load. Therefore, explanation for strengthening should lie in the micro-mechanisms.

In direct strengthening models, it has been[21-23] suggested that dislocations during their motion on glide planes would be obstructed by dispersoid particles. Dislocation thus obstructed can continue their motion by bending around the particles by Orowan mechanism[21] or modified Orowan mechanism[22]. The estimated yield values according to these mechanisms[21,22] are too low (below 10% of total yield strength) to account for the observed strengthening in Lead-base particulate composites.

Indirect strengthening of matrix by dispersoids can be expressed through Hall-Petch type[45,46] relationship:

$$\sigma_y = \sigma_i + k_y D^{-1/2} \qquad (4.2)$$

where σ_i and k_y are material constants and **D** is average grain diameter of matrix grains. σ_i is a measure of matrix frictional stress and k_y is a measure of grain boundary strength[81], unpinning stress for Frank-Read source in the adjacent grains[82] or stress to operate grain boundary dislocation sources[83]. Strengthening of the matrix can come through decrease in '**D**' or increase in σ_i and k_y factors. Particulate dispersoids can stabilise fine grain size, increase σ_i through dispersion inside the matrix grains or increase k_y by concentrating on the grain boundaries[83].

Using tensile yield strength and grain size data of the present investigation, plots have been obtained (as shown in Figure 4.1(a,b,c) showing relationship between σ_y and $D^{-1/2}$ in various composites tested at three different temperatures, viz. 28°C (RT), 100°C and 180°C. Similar plot has been obtained for pure Lead tested at 28°C (RT). From the plots, values of σ_i and k_y are determined and Hall-Petch type equations governing room temperature yield behaviour of various composites are obtained. The various values of σ_i and k_y for these composites at room temperature are summarised in Table 4.1. From the Table 4.1, it would be clear that for a given grain size, all the Lead base composites would be stronger than pure Lead either due to higher σ_i or k_y or both.

It is interesting to note that σ_i is considerably higher for P/M Lead (containing PbO) and Al_2O_3 containing

Lead base composites over that of pure Lead, whereas there is marginal gain due to Zn dispersoids in σ_i (Table 4.1). On the contrary, k_y values are improved to a large extent by Zn dispersoids over that of Lead (Table 4.1). Moreover, PbO and Al_2O_3 have an adverse effect on k_y. These observations can be rationalised on the following lines.

As far as σ_i is concerned, dispersoids would be effective in increasing its value, provided they are available within the grains. When the particles are within the matrix, it can give rise to Orowan type resistance[21] and resistance due to thermal stress field associated with dispersoids[15,79].

On the basis of micro-structure obtained in the present investigation, PbO and Al_2O_3 are partially available within the matrix, whereas Zn dispersoids are mostly at the grain boundaries. Further, the thermal residual stress field of compressive nature is associated with PbO and Al_2O_3 dispersoids, while in case of Zn dispersoids a thermal residual stress of tensile nature but of negligible amount is expected. As a consequence, there is a large contribution to σ_i in PbO and Al_2O_3 containing composites. Further, additional factors such as textural effects may also influence σ_i.

Since, k_y is related to the stress necessary to activate grain boundary sources of dislocations[83], accumulation of dispersoids at the grain boundaries would lead to

an increase in k_y. In Pb-Zn composites, Zn dispersoids are observed to be at the grain boundaries (Figure 3.3). Accordingly, k_y in these composites is significantly higher than that of pure Lead. In case of P/M Lead and Pb-Al$_2$O$_3$ though there is partial occupation of the boundaries by the dispersoid particles, k_y is adversely affected. The possible reason for such an effect lies in that PbO and Al$_2$O$_3$ being relatively much harder than the matrix, they would themselves act as dislocation generators[43] and bring the k_y value down.

σ_i is seen to decrease with increasing temperature of testing (Figure 4.2). This is expected because of its dependence on shear modulus of the matrix material which is temperature sensitive. In addition to this, thermal residual stress fields associated with PbO and Al$_2$O$_3$ are expected to decrease with increasing temperature and hence a more rapid fall in σ_i in P/M Lead and Pb-Al$_2$O$_3$ is expected as compared to that of Pb-Zn composites. The same is borne out by the present experimental results.

k_y is also observed to decrease with increasing test temperature. The drop in k_y of Pb-Zn composites is more rapid than that of P/M Lead and Pb-Al$_2$O$_3$ composites. As already mentioned, k_y is a measure of grain boundary resistance for generation of dislocations at grain boundaries[83]. The relative changes in k_y with temperature for various composites may be attributed to the corresponding change in grain boundary resistance offered to generate

dislocations. The decrease in shear modulus of Lead with
temperature is one factor that will decrease this grain
boundary resistance for dislocation generation. This would
lead to only moderate drop in k_y with temperature. In case
of hard particles like Al_2O_3 and PbO, the particles that
are at the grain boundaries can act as dislocation sources
and their ability to act as dislocation sources might not be
significantly affected by temperature. On the other hand,
in the case of softer dispersoid like Zn the dispersoid
particles would not aid the process of dislocation genera-
tion. Instead, these particles would act as obstacles to
dislocation generation due to their higher density at grain
boundaries. In Zn, the rate of drop in shear modulus with
temperature is considerable[84]. Accordingly, as the
temperature increases, the hardness of Zn dispersoid is
likely to fall rapidly and thus the effectiveness of Zn
particles in acting as barriers to dislocation sources at
grain boundaries is expected to decrease rapidly with
temperature. This may be the reason for rapid drop in k_y
with temperature in the case of Pb-Zn composites (Figure 4.2).

Increase in yield strength of Al_2O_3 containing
composites with increase in volume fraction of dispersoids
can be rationalised on the basis of expected increase in
σ_i parameter with the increase in dispersoid volume fraction.
However, the decrease in yield strength of Pb-Zn composites
cannot be rationalised on the basis of expected changes in

σ_i or k_y. The explanation for such apparently contradictory behaviour lies in the experimentally observed fact that recrystalised grain sizes of Pb-Zn composites are observed to be larger in comparison to Pb-Al$_2$O$_3$ composites (see Note below Table 3.7). The strength is lowered because of larger grain size obtained at greater volume fraction of Zn dispersoids.

4.4 Creep Behaviour of Lead-base Composites

The $\log \dot{\gamma}_s$ vs. $\log \tau_a$ plots shown in Figure 3.18 indicate the three distinct regions namely, zero creep rate, stress exponent region $n_a = 3$ and stress exponent region $n_a = 10$ for P/M Lead. It is observed that the stress exponents are modified to $n_e = 1$ and $n_e = 5.2$ in the steady state creep range for P/M Lead when internal stresses are taken into account (Figure 3.18). Similar qualitative behaviour for Pb-5 V/O Zn and Pb-5 V/O Al$_2$O$_3$ would be expected, although no internal stress measurements was done in these cases.

It is to be noted that, from the Arrhenius plots given in Figure 3.20 for P/M Lead, the observed apparent activation energies are 9.75 and 30 kcal/mol for regions of stress exponents of $n_a = 3$ and $n_a = 10$ respectively. If the effective stress is used to estimate the activation energy, the values would be lower than those obtained on the basis of applied stress. The stress exponent $n_e = 1$, is indicative

of four possible operative creep mechanisms. These are (i) Nabarro-Herring (N-H)[85], (ii) Coble[86], (iii) Harper-Dorn[87] and (iv) Grain boundary sliding (GBS)[88].

In case of Harper-Dorn creep[87] mechanism, creep rate is proportional to stress applied and activation energy is equal to that for self diffusion of the metal. In case of Lead, activation energy for self diffusion is 22.92 kcal/mol[60]. On the basis of measured activation energy (below 10.9 kcal/mol) in these Lead-base composites in low stress exponent region, the possibility of applicability of Harper-Dorn creep mechanism can be ruled out.

If Coble[86] or N-H[85] creep controls the creep behaviour, primary creep would be expected to be absent. However, there is considerable amount of primary creep exhibited in all the Lead-base composites. Moreover, estimated shear creep rates according to Coble and N-H mechanisms are below 10^{-9} sec^{-1} for the applied shear stress in the present investigation, whereas the observed creep rates in this region are above 10^{-7} sec^{-1}. Hence, both N-H and Coble creep mechanisms may also be excluded as operative mechanisms in this region. Thus, the operative mechanism is likely to be the grain boundary sliding (GBS). Since the grain sizes of these composites are relatively small, the GBS can possibly be an important mode of deformation at temperatures above 0.5 T_m.

The observed threshold stress in P/M Lead containing PbO and Pb-Al$_2$O$_3$ composites may also be a characteristic of GBS mode of deformation (Figure 3.18). Because of the presence of dispersed particles. mostly at or near the grain boundaries, there is a greater sliding resistance in comparison to a particle free boundary sliding[89] and the threshold stress may represent the minimum stress level below which sliding cannot occur. The threshold stress is observed to decrease with increasing temperature similar to other reported cases[36,90]. The absence of threshold stress in Pb-Zn composites may be due to softer nature of Zn dispersoid which is expected to offer much less resistance to sliding than other hard dispersoids.

In the higher stress exponent region the modified stress exponent is $n_e = \underline{5.2}$, in the steady state creep range of P/M Lead (Figure 3.18). Further, it is to be noted that the Arrhenius plots of Figure 3.20 for P/M Lead yield the activation energy value of 30 kcal/mol for higher stress exponent region in all cases. If the effective stress is used to estimate the activation energy, the values would be lower than those obtained on the basis of applied stress. The modified stress exponent on the basis of effective stress and the activation energies are in reasonable agreement with the dislocation climb model proposed by Ansell and Weertman[38].

Table 4.1

Values of σ_i and k_y for Lead-base
composites at room temperature

(Process IV)

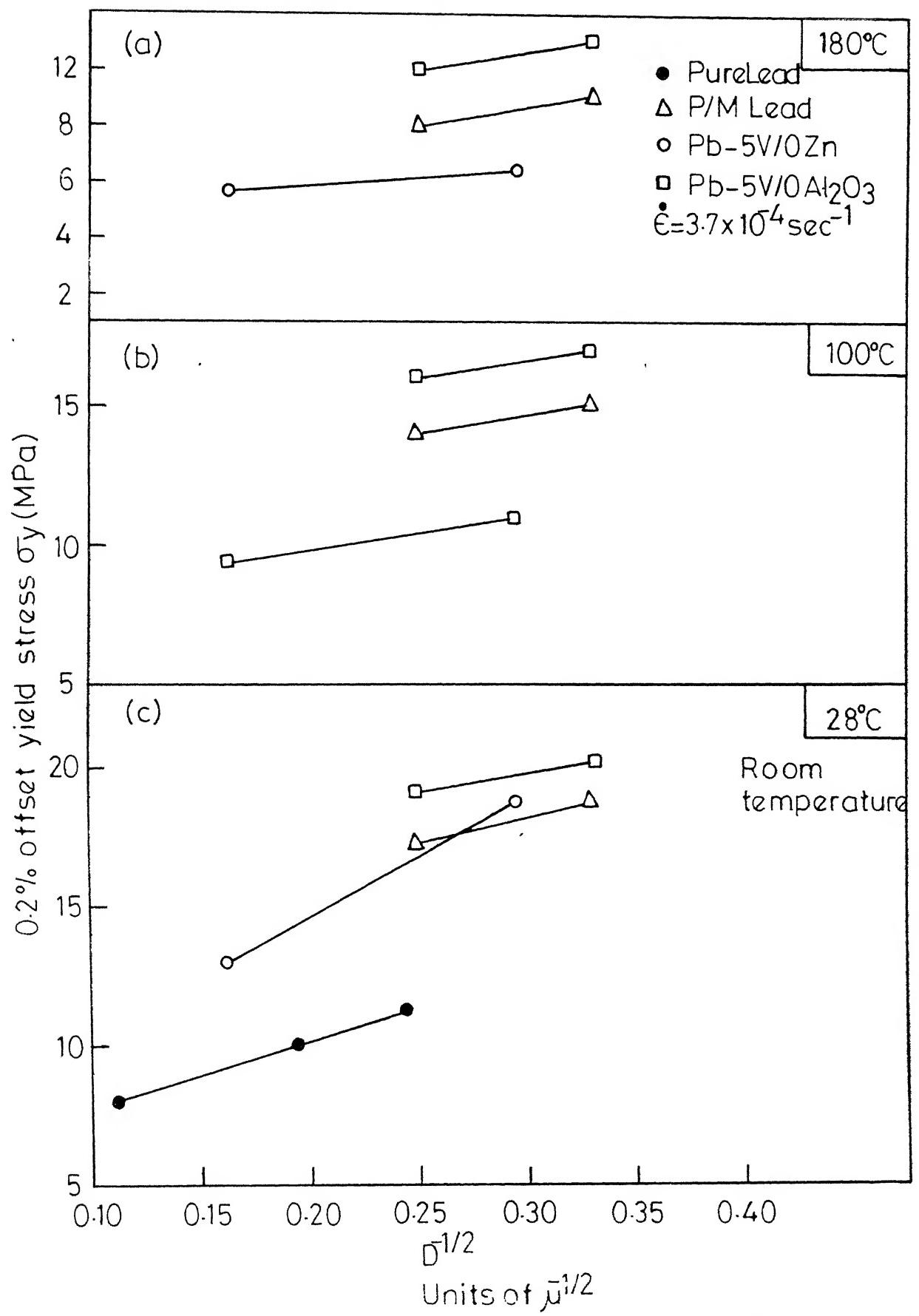| Material	σ_i (MPa)	k_y (Mpa $\mu^{1/2}$)
Pure Lead	5.2	21.0
P/M Lead	13.8	18.4
Pb-5 V/O Zn	7.0	46.0
Pb-5 V/O Al$_2$O$_3$	16.4	14.4

Fig. 4.1 – Relationship between yield stress (σy) and reciprocal square root of grain diameter D̄^{-1/2} of Lead and its composites.
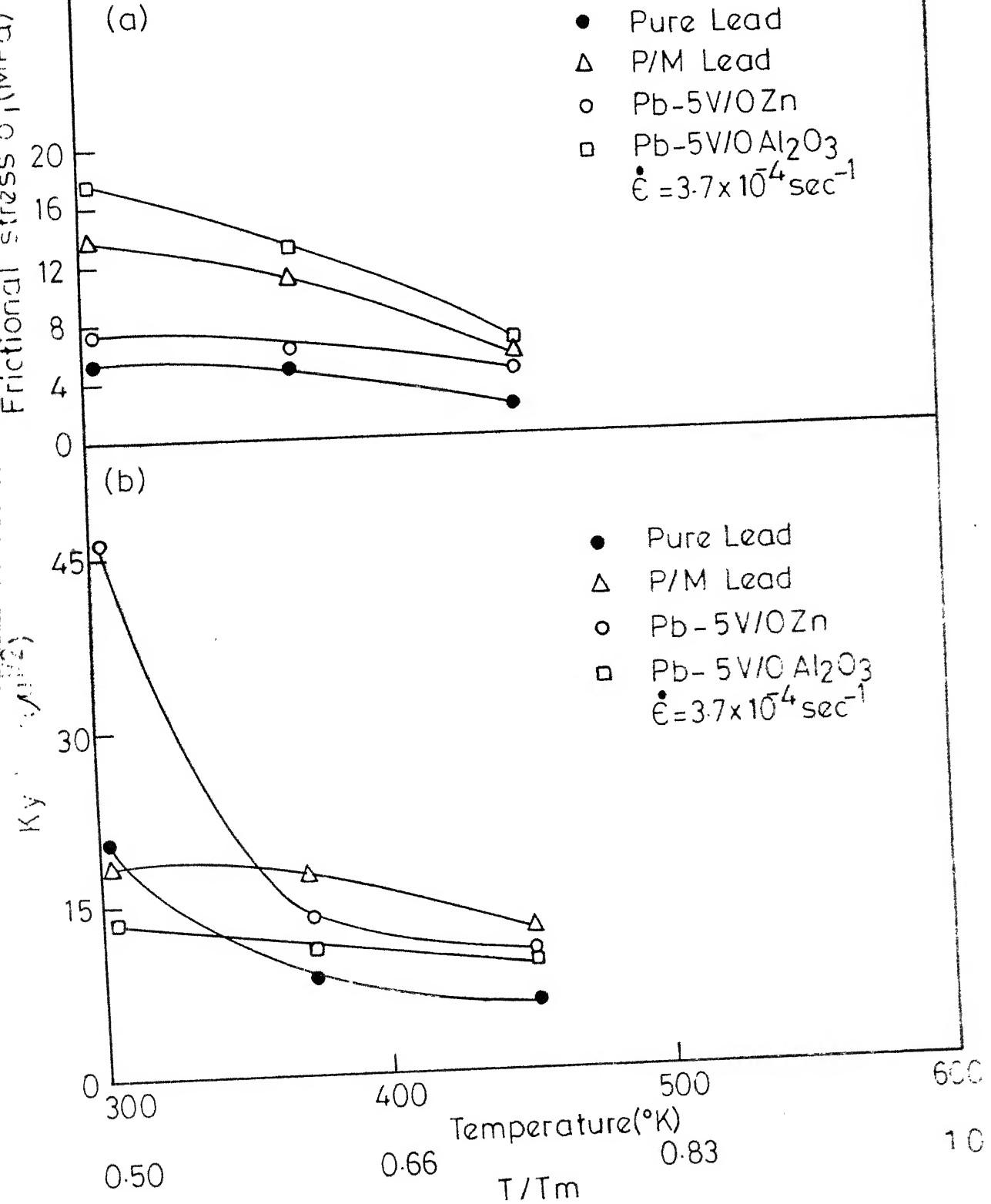
Fig. 4.2 -Temperature dependence of (a) σ_i (frictional stress) and (b) Ky in Lead and its composites.

CHAPTER V

CONCLUSIONS

1. The characteristics of Lead-base particulate composites prepared through P/M route are influenced significantly by the processing history. A suitable process design which include proper combination of mechanical working and thermal treatments provides the required homogeneity in terms of density in the final product. The density depends on the hardness of the dispersoid. Hard dispersoid will retain more porosity in the end product than the soft one.

2. The structural homogeneity of the composites is indicated by the extent of SD in the final product, especially at the nearly full density level. SD, the extent and sign of which depends upon the nature of dispersoid and processing history, may be treated as an additional characteristic for the dense (approaching theoretical density) P/M products.

3. In the dispersoid size range studied, all the Lead-base composites show strengthening over pure Lead (prepared through conventional route). Pb-Zn, P/M Lead and Pb-Al_2O_3 composites exhibit strengthening in increasing order. The observed strengthening or weakening with respect to P/M Lead is the outcome of indirect particle effects.

4. Threshold stress for steady state creep is observed in P/M Lead and Pb-5 V/O Al_2O_3 composites below 150°C, whereas it is absent in Pb-5 V/O Zn composites in the same temperature range. The threshold stress, thus, depends on nature of the dispersoid and temperature.

5. In the creep of Lead-base composites, high and low stress exponent regions with corresponding activation energies have been observed. In the low stress exponent region, grain boundary sliding appears to be the rate controlling mechanism, whereas climb controlled dislocation creep is the operative mechanism in the other region.

REFERENCES

(1) E.A. Bloch, Met. Review, 6, 193 (1961)

(2) N.J. Grant, Prog. in Powder Met., 16, 99 (1960)

(3) D.L. Wood, Trans. AIME, 215, 925 (1959)

(4) R.A. Rapp, "Oxide dispersion strengthening" Conf. Bolton Landing, New York, Pub. by Gordon and Breach, 539 (1968)

(5) O. Preston and N.J. Grant, Trans. AIME, 221, 164 (1961)

(6) A. Gatti, Trans. AIME, 215, 753 (1959)

(7) R.W. Fraser, B. Meddings, D.J.I. Evans, Int. Powder Met. Conf. No. 30(F), 1965.

(8) K.M. Zwilsky and N.J. Grant, Trans. AIME, 221, 371 (1961)

(9) J.S. Benjamin, Sci. Amer., 234, 40 (1976)

(10) J.A. Lund, D. Tromans, and B.N. Walker, Lead Powder Met. Project LM-8, p. 16, 1968.

(11) J.A. Lund, D. Tromans, and B.N. Walker, ibid. p. 13, 1968.

(12) R. Murphy and N.J. Grant, Powder Met., 10, 1 (1962)

(13) C. Nishimatsu and J. Gurland, Trans. ASM, 52, 469 (1960)

(14) J. Wambold, in Cermets Edited by J.R. Tinklepaugh and W.B. Crandell, Reinhold, Pub. Corp., New York, 122 (1960)

(15) F.R.N. Nabarro and B. Luycky, Proc. of 2nd Int. Conf. on the Strength of Metals, ASM, Ohio, 1968.

(16) B.I. Edelson and W.M. Baldwin Jr., Trans. ASM., 55, 230 (1962)

(17) R.J. Towner, Metal Prog., 73, 70 (1958).

(18) J.G. Rasmussen and N.J. Grant, Powder Met., 8, 92 (1965)

(19) K.M. Zwilsky and N.J. Grant, Trans. AIME, 221, 205 (1961).

(20)   A. Gatti, Powder Met., 8, 64 (1965)

(21)   E. Orowan, "Symposium on Internal Stresses in Metals",
         London (Inst. Metals), 451 (1948)

(22)   M.F. Ashby, Acta Met., 14, 679 (1966)

(23)   G.S. Ansell and F.V. Lenel, Acta Met., 8, 612 (1960)

(24)   A.K. Mukherjee and J.W. Martin, J. Less Common Metals,
         2, 392 (1960)

(25)   V.A. Tracey and D.K. Worn, Powder Met., 10, 34 (1962)

(26)   R.J. Towner, Trans. AIME, 230, 505 (1964)

(27)   B.A. Wilcox and R.I. Jaffe, Japan Inst. of Metal, 9
         (Supplement), 575 (1968)

(28)   R.J. Olsen and G.S. Ansell, Trans. ASM., 62, 711 (1969)

(29)   J.E. Franklin, G. Judd, and G.S. Ansell, The
         Microstructure and Design of Alloys, Proc. of 3rd Int.
         Conf. on the Strength of Metals and Alloys, Vol. 1,
         Paper 70, 1973.

(30)   G.C. Reed and W.L. Schalliol, J. Metals, 16, 175 (1964)

(31)   N.E. Ryan and S.T.M. Johnstone, Less Common Metals, 8,
         159 (1965)

(32)   F. Seitz, Adv. Phys., 1, 43 (1952)

(33)   B.A. Wilcox and A.H. Clauer, Trans. AIME, 236, 570
         (1966)

(34)   B.A. Wilcox, A.H. Clauer, and W.S. Mccain, Trans. AIME,
         239, 1791 (1967)

(35)   C.L. Meyers, J.C. Shyne, and O.D. Sherby, J. Aust. Inst.
         Met., 8, 171 (1963)

(36)   J.H. Hausselt and W.D. Nix, Acta. Met., 25, 1491 (1977)

(37)   J.J. Petrovic and L.J. Ebert, Met. Trans., 4, 1301
         (1973)

(38)   G.S. Ansell and J. Weertman, Trans. Met. Soc. AIME,
         215, 838 (1959)

(39)   C.N. Aliquist and W.D. Nix, Scripta Met., 3, 679 (1969)

(40)   P.W. Davies, G. Nelmes, K.R. Williams, and B. Wilshire,
         Met. Sci. J., 7, 87 (1973)

(41)   R. Lagneborg and B. Berman, Met. Sci. J., 10, 20 (1976)

(42)   W.H. McCarthy, J.C. Shyne, and O.D. Sherby, Trans. ASM,
         62, 117 (1969)

(43)   G.R. Edwards, T.R. McNelley, and O.D. Sherby, Phil. Mag.,
         32, 1245 (1975)

(44)   Shu-En Hsu, G.R. Edwards, J.C. Shyne, and O.D. Sherby,
         J. Mat. Sci., 12, 131 (1977)

(45)   E.O. Hall, Proc. Roy. Soc., B64, 747 (1951)

(46)   N.J. Petch, J.I.S.I., 174, 25 (1953)

(47)   W.T. Read, Dislocations in Crystals, p. 85, McGraw-Hill, N.Y.,
         (1953)

(48)   S.L. Mannan and P. Rodriguez, Acta. Met., 23, 221 (1975)

(49)   D.J.I. Evans, H.R. Huffman, and J.P. Warner, 59(4), 105
         (1964)

(50)   S.T. Gazzard, D.H. Roberts, J.C. Moore, and N.A. Ratcliff,
         Lead 65, Proc. of Second International Conf. on Lead,
         Arnhem, Pergamon press, Oxford, p. 17 (1965)

(51)   D.H. Roberts and N.A. Ratcliff, Metallurgia, 70, 223
         (1964)

(52)   J.A. Lund, D. Tromans, and B.N. Walker, Lead Powder
         Met., Project LM-8, p. 24, 1968.

(53)   J.A. Lund, D. Tromans, and B.N. Walker, ibid. p.44, 1968.

(54)   J.A. Lund, D. Tromans, and B.N. Walker, ibid. p. 25, 1968.

(55)   J.A. Lund, E.G. Van Tiesenhausen, and D. Tromans, Lead 65,
         Proc. of Second International Conf. on Lead, Arnhem,
         Pergamon Press, Oxford, p. 7 (1965)

(56)   R. Kossowsky and N. Brown, Trans. Met. Soc. AIME, 233,
         1389 (1965)

(57)   G.H. Reynolds, Scripta Met., 8, 781 (1974)

(58)   R.C. Gifkins and K.U. Snowden, Trans. Met. Soc. AIME, 239, 910 (1967)

(59)   M.L. Vaidya, K. Linga Murthy and J.E. Dorn, Acta Met., 21, 1615 (1973)

(60)   F.A. Mohamed, K.L. Murthy, and J.W. Morris, Jr., Met. Trans., 4, 935 (1973)

(61)   H.A. Kuhn, "Powder Metallurgy Processing New Techniques and Analysis", Ed. by H.A. Kuhn and A.Lawley, Academic Press, N.Y., p. 99 (1978)

(62)   T. Sheppard and A. Greasky, Powder Met., 3, 155 (1978)

(63)   A.G. Metcalfe, "Composite Materials", Ed. by A.G. Metcalfe, Academic Press, N.Y., p. 20 (1974)

(64)   J.S. Hirchhorn, "Introduction to Powder Metallurgy", American Powder. Met. Inst., Princeton, New Jersy, p. 245, 1969.

(65)   J.S. Hirchhorn, ibid., p. 162, 1969.

(66)   W.H. McCarthy, J.C. Shyne, and O.D. Sherby, Trans. ASM, 62, 117 (1969)

(67)   A. Orlova, K. Milica, and J. Cadek, Z. Metalk., B63, H-2, 89 (1972)

(68)   M.F. Ashby and K.T. Aust, Acta Met., 15, 405 (1967)

(69)   M.F. Ashby and R.M.A. Centamore, Acta Met, 16, 1081 (1968)

(70)   M.F. Ashby, Scripta Met., 3, 843 (1969)

(71)   D. Kalish and M. Cohen, Trans. ASM, 62, 353 (1969)

(72)   J.D. McClelland, J. Amer. Ceram. Soc., 44(10), 526 (1961)

(73)   J.R. Patel and M. Cohen, Acta Met., 1, 531 (1953)

(74)   J.P. Hirth and M. Cohen, Met. Trans., 1, 3 (1970)

(75)   D. Kalish and M. Cohen, Trans. ASM, 62, 353 (1969)

(76)   J.P. Hirth and M. Cohen, Met. Trans., 1, 3 (1970)

(77) M.D. Merz, Met. Trans. 4, 1186 (1973)

(78) D. Griggs and W.B. Miller, Bull. Geol. Soc. Amer. 62, 853 (1951)

(79) H.T. Carton, "Modern composite materials", Ed. L.J. Broutman and R.H. Crock, Addison Wesley Publishing Company, Mass., p. 30 (1967)

(80) Hand book of Chemistry and Physics, Ed. by Hodgeman, C.D. et al, Chemical Rubber Pub. Co., Cleveland, 2275 (1971)

(81) J.D. Eshelby, F.C. Frank, and F.R.N. Nabarro, Phil. Mag. 42, 351 (1951)

(82) A.H. Cottrell, Trans. Met. Soc. AIME 212, 192 (1958)

(83) J.C.M. Li, Trans. Met. Soc. AIME 227, 239 (1963)

(84) W. Koster, Z. Metallk. 39, 1 (1948)

(85) F.R.N. Nabarro, Ref. Conf. Strength of Solids, Phys. Soc. London, 1948

(86) R.L. Coble, J. Appl. Phys. 34, 1679 (1963)

(87) J.G. Harper and J.E. Dorn, Acta Met. 5, 654 (1957)

(88) G.B. Gibbs, Mem. Sci. Rev. Met. 62, 775 (1965)

(89) C. Hammond and J. Nutting, Metal Sci. 11, 474 (1977)

(90) B. Burton and W.B. Beere, Metal Sci. 12, 71 (1978).

PUBLICATIONS

Based on part of the work presented in the thesis, following two articles have already been published:

(1)   "Preparation and Characterisation of Lead-base P/M Composites" - Trans. Powder Met. Association of India, 6 (1979).

(2)   "Strength Differential (SD) Effect in Sintered Lead-base Particulate Composites" - Proceedings of Symposium on Sintering and Sintered Products, Oct. 29-31, 1979, BARC, Trombay (in Press).